DEVELOPMENT AND TESTING OF A FLUOROMETRIC METHOD AND INSTRUMENT BASED ON THE 2',7' DICHLORODIHYDROFLUORESCIN ASSAY FOR THE MEASUREMENT OF REACTIVE OXYGEN SPECIES

A Thesis
Presented to
The Academic Faculty

by

Laura Emily King

In Partial Fulfillment
of the Requirements for the Degree
Master of Science in the
School of Earth and Atmospheric Sciences

Georgia Institute of Technology
December 2012

DEVELOPMENT AND TESTING OF A FLUOROMETRIC METHOD AND INSTRUMENT BASED ON THE 2',7' DICHLORODIHYDROFLUORESCIN ASSAY FOR THE MEASUREMENT OF REACTIVE OXYGEN SPECIES

Approved by:

Dr. Rodney Weber, Advisor
School of Earth and Atmospheric Sciences
Georgia Institute of Technology

Dr. Armistead (Ted) Russell
School of Civil and Environmental Engineering
Georgia Institute of Technology

Dr. Michael Bergin
School of Civil and Environmental Engineering
Georgia Institute of Technology

Date Approved: November 8, 2012

TABLE OF CONTENTS

ACKNOWLEDGEMENTS

This work was supported by USEPA grant RD83479901. Its contents are solely the responsibility of the author and do not necessarily represent the official views of the USEPA. Further, USEPA does not endorse the purchase of any commercial products or services mentioned in the publication.

This research was also made possible in part by collocating field deployments with sites operated by Atmospheric Research and Analysis (ARA) as part of the Southeastern Aerosol Research and Characterization (SEARCH) network of monitoring stations, which are funded by in part by the Electric Power Research Institute (EPRI) and the Southern Company. This work does not necessarily represent the views of any of the above parties, nor do they endorse any of the commercial products mentioned within this text.

Many people were partially responsible for the results described within this thesis, but the most important person is Dr. Rodney Weber, who, beyond everything else, said yes when he could have said no.

LIST OF TABLES

LIST OF FIGURES

SUMMARY

An online, semi-continuous instrument to measure both total and gas phase atmospheric reactive oxygen species (ROS) and determine the concentration of ROS in the particle phase (ROS(p)) was developed. This instrument was based on a fluorescent probe for quantifying ambient ROS, specifically 2'7'-dichlorodihydrofluorescin, or DCFH probe. Together with a catalyst, peroxidase from horseradish (HRP), this compound reacts with various forms of ROS and produces DCF-. When DCF- is excited by light at a wavelength of 485 nm, it fluoresces at 530 nm. This probe was analyzed for sensitivity to a variety of offline and online parameters for efficient use in a field instrument, including concentration, volumetric ratio of reagents to sample, incubation temperature, reaction time and reagent age.

The ROS(p) instrument measures the peak light intensity at 530 nm to determine ambient ROS concentrations. ROS particles and gases are collected in a mist chamber in a nebulized mist. The instrument alternates measurements of ROS(p+g), or ROS(tot) by means of an inline filter.. Fine ($PM_{2.5}$) (ROS(p) is determined by subtraction of the ROS(g) concentration from the ROS(tot), as the ROS(g) signal could not be excluded. This instrument was tested at the Southeastern Aerosol Research and Characterization (SEARCH) Jefferson Street site February 2012 in central Atlanta and during the first phase of the Southern Center for Air Pollution and Epidemiology study during the summer (May-July) of 2012 at urban and rural sites in the metropolitan Atlanta and surrounding region.

Concentrations of ROS(p) determined from this instrument were often below limit of detection. Average concentrations of ROS(p) were found to be 0.25 nmol/m^3 in urban

Atlanta (Jefferson St. and Georgia Tech), and 0.15 nmol/m^3 in Yorkville, a rural site. A side by side comparison of this method with a filter collection method was made in July. The average ROS(p) offline concentrations were 0.15 nmol/m^3. These concentrations were comparable to the online average concentrations of 0.21 nmol/m^3 for the same period of time. This average and the majority of the measurements comprising it is dominated by the high limit of detection. Other ambient ROS(p) filter studies had generally higher concentrations of ROS(p) (Hung and Wang 2001; Venkatachari, Hopke et al. 2005; Venkatachari, Hopke et al. 2007), as did an online instrument (Wang, Arellanes et al. 2010), though it also reported a good agreement with simultaneous filter assessments. The ROS instrument as constructed and operated is an efficient way to conduct ROS(p) measurements at the level of a filter study while reducing the labor intensive filter collection and extraction.

In order for this instrument to be successful at measuring ambient ROS in the particle phase, the removal of the gas phase from the current sampling scheme is critical as the ROS(g) concentrations are over 90% of the measured ROS. Either a new collection method that retains or concentrates ROS particles but excludes the gas phase must be employed or a consistent and highly efficient gas removal system must be added to the existing setup. It is possible that a variant on the coating and application of the common ROS removal compounds in denuders could more consistently and efficiently remove the ROS(g) concentrations.. The system as currently operable is best suited for source measurements, including biomass burning plumes or fresh exhaust to capture immediate formation.

CHAPTER 1

INTRODUCTION

Reactive oxygen species (ROS) are a family of odd oxygen compounds including hydrogen peroxide, superoxide radical, peroxy radical, hydroxyl radical, hypochlorous acid and other organic hydroperoxides. These compounds maintain the natural oxidative capacity of the troposphere both in terms of oxidative potential and as a reservoir for other oxygen radical species. Higher concentrations of ROS are produced in more highly polluted environments and are additionally responsible for elevation of ozone concentrations.

ROS have been shown to have a significant impact on human health, contributing to both cellular and system oxidative stress which can lead to cardiovascular disease, accelerated aging and pulmonary damage (Rothe and Valet 1990; Sioutas, Delfino et al. 2005; Vidrio, Phuah et al. 2009; Sugamura and Keaney 2011). ROS may be generated within cells from reactive or nonreactive compounds by both regular biologic processes (Sugamura and Keaney 2011) and from exposure to compounds with an increased oxidative capacity (Verma, Shafer et al. 2010). Ambient ROS may also enter the body primarily through the airways and deposit in the upper respiratory tract (large particles and gases) or penetrate further into the lungs (fine and ultrafine particulate matter). Due to the short lifetimes of ROS in the atmosphere, on the order of minutes and hours for radicals to less than two days for larger compounds such as hydrogen peroxide and methylhydroperoxide (Reeves and Penkett 2003), the measurement of particle phase ROS has a high degree of uncertainty.

The Georgia Institute of Technology (Georgia Tech) and Emory proposed and were funded by EPA for a Clean Air Research Center (CLARC) named SCAPE: the Southern Center for Air Pollution and Epidemiology. This center is comprised of four projects and three cores. The first project (Project 1) will comprehensively measure and characterize gas/particle mixtures of air pollutants for this Center's multiscale air quality model validation, health impact assessments and source/process studies. The data will complement and extend current pollutant observations across multiple scales greatly enhancing existing air quality data sets to include more exotic species for retrospective and prospective health studies in other urban settings.

A focus of these new measurements will be on identifying and quantifying agents that have been implicated in causing oxidative stress**.** Within Project 1, the Center proposed an online instrument to measure and broadly speciate aerosol Reactive Oxygen Species (ROS) to be developed for stationary and in-vehicle measurements, and included in an instrumentation package focused on semi-continuous measurements of trace gas and aerosol species. Measurements are to be taken across a variety of locations in different seasons to characterize spatial, temporal and chemical distributions, sources, and physicochemical processes or linkages between components of gas/particle pollutant mixtures implicated in adverse health outcomes. Species to be measured include particle phase ROS, redox active metals, quinones, PAHs, speciated carbonaceous compounds, and ultrafine, fine and coarse particles, along with gas-phase oxidants, VOCs, NO_x, and CO. Specifically, from a biologically based perspective, these measurements will be

used to assess the role of ROS and other oxidants in the biological activities relevant to oxidative stress mediated responses.

CHAPTER 2:

BACKGROUND

2.1 ROS Composition and sources

Reactive oxygen species, collectively known as ROS, are a family of oxygen compounds in the atmosphere characterized by high oxidative potentials and short lifetimes. This group includes nonradical species such as hydrogen peroxide (H_2O_2), hypochlorous acid (HOCl), and organic hydroperoxides, as well as radicals such as hydroxyl radical (OH), HO_2 and peroxy radicals (RO_2). Peroxy radicals are particularly important components for ozone production in low NOx environments, making their presence in the troposphere of general interest (Seinfeld and Pandis 2006). ROS are an important part of the troposphere's oxidative capacity, with peroxides serving as reservoirs for even shorter lived radicals such as the hydroxyl radical, OH, and the greater family of hydrogen oxide radicals (HO_x = H + OH +HO_2) (Jacob 1999), in both the clean and polluted troposphere.

While ROS are comprised of more than twenty distinct species without counting all potential forms of organic hydroperoxides (Gomes, Fernandes et al. 2005), general ROS tropospheric chemistry can be described with the formation and destruction of the more common species such as hydroxyl radical and peroxyl radical (Reeves and Penkett 2003), the primary reservoir molecule hydrogen peroxide, and HO_2.

Hydrogen peroxide from HO_2

$HO_2 + HO_2 + H_2O \rightarrow H_2O_2 + O$

HO_2 from ozone photolysis

$O_3 + h\nu \rightarrow O(1D) + O_2$
$O(^1D) + H_2O \rightarrow 2OH$
$OH + CO + O_2 \rightarrow HO_2 + CO_2$

Methyl hydroperoxide (CH_3OOH or MHP) is the dominant hydroperoxide over ocean waters:

$CH_4 + OH + O_2 \rightarrow CH_3O_2 + H_2O_2$
$CH_3O_2 + HO_2 \rightarrow CH_3OOH + O$

Reaction of NO with these peroxyl radicals is much faster than reacting with other peroxyl radicals, in higher NO environments these reactions will dominate (Reeves and Penkett 2003).

$NO + HO_2 \rightarrow NO_2 + OH$
$OH + CH_3O_2 + O_2 \rightarrow NO_2 + CH_2O + HO_2$

Hydrogen peroxide and MHP are lost via photolysis and reaction with OH.

$H_2O_2 + h\nu \rightarrow 2OH$
$CH_3OOH + h\nu + O_2 \rightarrow CH_2O + HO + HO_2$
$H_2O_2 + OH \rightarrow H_2O + HO_2$
$CH_3OOH + OH \rightarrow CH_3O_2 + H_2O$

These general gas phase reactions illustrate the basic principles by which ROS are generated in the troposphere. From a health impact perspective, most interested is in compounds that are in excess of their natural concentrations and in locations where there will be increased exposure to humans leading to adverse health effects. ROS in the particle phase represents a potentially greater health threat to humans given the greater potential for particles to penetrate the airways and deposit deeper in the lungs. Overall, little is known regarding the mechanisms by which ROS are incorporated into the particle

phase. Associations with fresh particle generation such as welding fumes (Antonini, Clarke et al. 1998) and silica dust (Hung and Wang 2001) have been established.

2.2 Exposure pathways and health effects of ROS

Highly reactive compounds, such as ROS, when introduced into a biological system have a strong tendency to disrupt the electrochemical balance, depending on factors such as the amount of ROS introduced or produced within the system, the location of the introduction or production of the reactive species, the duration of the insult and a host of other factors, many of which have yet to be ascertained in nature as well as in scope (Rothe and Valet 1990; Barrett, DeGnore et al. 1999; Morgan, Davis et al. 2001; Squadrito, Cueto et al. 2001; Oberdörster 2004; Xia, Kovochich et al. 2006; Sugamura and Keaney 2011). Human exposure to ROS can occur by a number of known routes. ROS associated with gaseous or particulate pollutants generated in the atmosphere may be transported into the respiratory system. Their deposition generates adverse effects within cells of that location. Components associated with aerosol particles may also be deposited and result in either a direct or indirect generation of ROS intracellularly, in which the oxidative stress may not be limited to the immediate area of deposition. The following section details the sources and potential mechanisms that lead from atmospheric particulate matter to oxidative stress in the body and the ways in which they can be quantified.

2.3 Techniques for quantifying ROS

2.3.1 Ambient ROS: Direct exposure to oxidizing species

It is well established that reactive and oxidizing species are detrimental to biological systems in a wide variety of ways, including disrupting protein pathways, increasing the breakdown of key cellular structures and leading to the eventual death of individual cells, prior to which large amounts of cellular stress translates into wider systemic stress in organisms (Antonini, Clarke et al. 1998; Barrett, DeGnore et al. 1999; Squadrito, Cueto et al. 2001; Sugamura and Keaney 2011). Atmospheric exposure to ROS can occur either in the gas or particle phase. Unlike ozone, a weakly soluble oxidizing gas with well characterized health effects, gas phase ROS is most likely to be removed in the upper mucus membranes (Kao and Wang 2002), whereas other studies (Pope, Thun et al. 1995) have demonstrated the ability of fine particles to penetrate further into the lungs and deposit in the alveoli.

Atmospheric studies to measure ambient ROS have focused primarily on gas phase measurements (Reeves and Penkett 2003; Klippel, Fischer et al. 2011) typically using fluorescent probes, while the particle measurements have primarily been filter extractions using the same probes (Hung and Wang 2001). Fluorescent probes such as 2',7', dichlorofluorescin (DCFH), Amplex Red, p-hydroxyphenylacetic acid (POHPAA) and others have been adapted from their use in intracellular ROS measurements for direct measurements in the atmosphere. Various ROS will oxidize these probes, which then fluoresce at specific wavelengths when excited. Fluorescent probes are most often chosen for their fast response rates, linear response to varying ROS concentrations and either dedicated response to a particular compound (e.g. Amplex Red) (Zhou, Diwu et al.

1997) or lack of chemical specificity (e.g. DCFH) (LeBel, Ischiropolous et al. 1992). These filter-based particle studies have found ROS (specifically hydrogen peroxide) partitioning to the particle phase can be orders of magnitude higher than predicted by Henry's Law (Hasson and Paulson 2003; Arellanes, Paulson et al. 2006). Given the ability for the particle phase to penetrate further into the lungs, this suggests that the impact of particulate ROS may have a greater impact than previously thought.

The overall findings of measurements of ambient ROS have shown some associations with other atmospheric species. Ambient particle phase ROS is positively correlated with both Fe concentration and other transition metals (See, Wang et al. 2007). There are also positive correlations with overall organic concentrations (Wang, Arellanes et al. 2010). There is a weak correlation between ROS and ozone (Venkatachari, Hopke et al. 2005) as measured in bulk atmospheric aerosols. A summary of these findings is presented below in Table 2.3.1-1.

Table 2.3.1-1. Summary of findings of studies measuring ambient ROS concentrations.

Method	Major Findings	Source and Phase of ROS	References
ROS Concentration via probe oxidation (DCFH, Amplex Red, etc.)	Hydroperoxide concentrations, mainly H2O2, exceed Henry's law by several times	Ambient atmosphere [both gas and particles (PM10 and 2.5)]	(Hasson and Paulson 2003)
	OH formation rates correlated with dissolved Fe and organics	Bulk ambient aerosol	(Arakaki, Kuroki et al. 2006)
	H2O2 concentrations higher than Henry's law, especially for coarse particles, concentrations in both fine and coarse modes highest by freeway	Ambient atmosphere [both gas and particles (PM10 and 2.5)]	(Arellanes, Paulson et al. 2006)
	ROS concentrations correlated with transition metals	combustion generated PM (fine)	(See, Wang et al. 2007)
	ROS concentrations (specifically measured by DCFH) moderately correlated with photochemistry (via ozone concentrations)	ambient aerosols	(Venkatachari, Hopke et al. 2005)
	Hydrogen peroxide concentration in the coarse mode correlated with (and potentially generated by) transition metals, but not quinones	coarse mode ambient aerosol	(Wang, Arellanes et al. 2010)

A potential drawback to the findings briefly summarized above is that all of the studies have used a bulk collection of particles, in solutions or on filter materials, and so those filter extracts or solutions have the potential to include particles that would generate ROS in solution that did not previously exist in the ambient form, creating a positive bias. Filter based studies, particularly for such reactive compounds as ROS, are also limited by the hours-long lifetimes of ROS particles, which have been hypothesized to result in the underprediction of concentrations even with near-immediate extraction and analysis of filters (Hung and Wang 2001). Most filter studies also report not only high but variable blank concentrations (Hung and Wang 2001; Venkatachari, Hopke et al. 2005; Venkatachari, Hopke et al. 2007).

Some preliminary results exist for an online method to measure particle phase ROS, reporting similar concentrations to those from certain filter studies (Venkatachari

and Hopke 2008; Wang, Hopke et al. 2011). This instrument couples the particle-into-liquid-sampler (PILS) with a flow system that mixes DCFH and peroxidase from horseradish (HRP) with the PILS sample stream (Venkatachari and Hopke 2008), the theory of which is described later here. After utilizing mixing elements to combine and sufficiently react the sample ROS with the fluorescent reagents, the sample is measured using a spectrometer. Results from a brief field operation (Wang, Hopke et al. 2011) showed an average of 8.3 ± 2.2 nmol hydrogen peroxide equivalents per meter cubed of air (nmol/m^3). This study, conducted over August 12-18, 2009, in Rochester, NY, also indicated a a diurnal trend in ROS(p) with an increase in daytime concentrations, as well as higher values on weekdays than on weekends. These values reported also exceeded ambient values found on filters in previous studies in the USA and Taiwan (Hung and Wang 2001; Venkatachari, Hopke et al. 2005; Venkatachari, Hopke et al. 2007). These results would appear to indicate that ROS loss from ambient filters is a factor improved upon using a continuous online system with virtually no delay between collection and analysis.

2.3.2 Nonreactive species oxidizing cellular antioxidants (oxidative potential)

Outside of the immediate impact from exogenous ROS on the lungs and cardiovascular system, other atmospheric aerosol components have been shown to create similar effects without being classified as ROS themselves. Redox active compounds are nonreactive compounds with a high oxidative potential that proceed to oxidize cellular antioxidants, thus reducing the cell's regular ability to manage other oxidizing processes. Many of these compounds are known and quantifiable fractions of aerosols, meaning that

an increased exposure could lead to a similarly increased intracellular load. The removal via oxidation of cellular antioxidants such as glutathione and ascorbic acid allows other cellular ROS to work unchecked, similar to an overload from ambient ROS.

One such assay developed to measure this particular pathway is known as the DTT (dithiothreitol, $HSCH_2(CH(OH))_2CH_2SH$) assay. The schematic shown in Figure 2.3.2-1 shows the reaction mechanism between DTT and the representative PM constituents, resulting in the measurement of its rate of consumption (adapted from Sameenoi, Koehler at al. 2012).

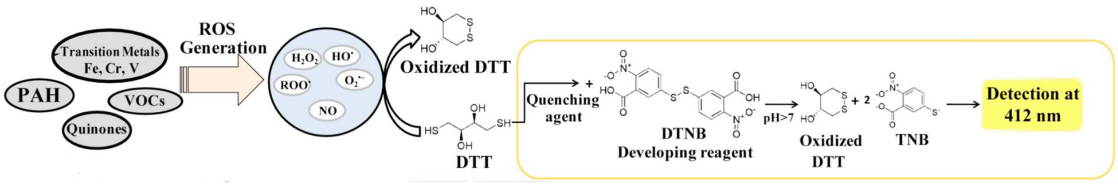

Figure 2.3.2-1: Schematic representing the reaction mechanism of DTT with ROS generating compounds and subsequent quantification of consumption rate.

In this assay, ambient particles are suspended in a buffered solution with DTT. Over time, DTT is consumed via reaction with the redox active compounds, the consumption of which is measured at various time points by the addition of a thiol reagent, 5,5' dithiobis-2-nitrobenzoic acid (DTNB). Concentrations are determined by a measurement of absorption at 412 nm (Kumagai, Koide et al. 2002). This reaction and the subsequent measurements of DTT consumption are somewhat time consuming given the rate of reaction for each sample and require multiple points of interaction with the extract. DTT and its subsequent consumption are a surrogate for the assumed oxidation of various cellular thiol antioxidants, in particular glutathione.

Research has shown that the DTT assay is primarily associated with organic oxidative components given the lack of impact on the assay from the addition of metal chelators (Cho, Sioutas et al. 2005; Ayres, Borm et al. 2008). However, more recent work suggests that metals are the more dominant species, emphasizing that the correlations observed between higher concentrations of WSOC or PAHs are not necessarily the specific causer of increased DTT consumption (Charrier and Anastasio 2012) .

The DTT assay is significantly more complex than the more direct measurement of ambient ROS, requiring a controlled environment, more chemical and buffer additions at specific time intervals and above all, a larger amount of overall reaction time limiting sample/analysis rates. However, such a measurement technique is able to provide different information on the total potential impact atmospheric components exposure, and lead to conclusions on the mechanisms that connect exposure, uptake and final oxidative stress.

Two other assays of note exist for the measurement of this type of oxidative potential from particulate matter, but are still in the development stages in terms of both analytical methodology and field use. One assay utilizes dihydroxybenzoate (DHBA) redox activity as a surrogate for the consumption of ascorbate within cells. The general pathway behind the measurement of redox active compounds is the same as with DTT, but the generated and measured product in this case is the hydroxyl radical, which requires quantification via HPLC (Ayres, Borm et al. 2008). Unlike DTT, DHBA has a marked sensitivity to transition metals as opposed to quinones and other organics based on its retardation by metal chelators. The second assay of this nature uses a slightly

different pathway than the previous two, in which glyceraldehyde-3-phosphate dehydrogenase (GAPDH) is inactivated in a permanent fashion via electrophilic covalent bonding to compounds such as acrylonitrile and some quinones. As GAPDH is another regular intracellular antioxidant, the measurements of its inactivation would assist in filling gaps in the overall understanding of the contribution of these particles on oxidative stress from ambient particles, but protocols for this type of assessment are still in progress (Ayres, Borm et al. 2008).

Table 2.3.2-1 summarizes the current findings of relevant studies using these probes and the relevant correlations to other atmospheric compounds.

Table 2.3.2-1. Summary of findings of studies measuring ambient particle oxidative potential

Method	Activity Correlations	Source of Particles	References
DTT Assay	Activity correlated with EC, OC, benzoperylen.	Ambient Aerosol (coarse, fine and ultrafine) at different sites in Los Angeles	(Cho, Sioutas et al. 2005)
	Activity correlated with PAHs content of PM and also with the HO-1 (hemeoxygenase - an indicator of cellular oxidative stress).	Ambient Aerosol (coarse, fine and ultrafine) at different sites in Los Angeles	(Li, Sioutas et al. 2003)
	Activity correlated with adjuvant effects of PM (allergic sensitization) in mice	Ambient fine and ultrafine aerosol in Los Angeles	(Li et al., 2009)
	Activity correlated with WSOC (emitted from biomass burning)	Ambient fine (<2.5 um) aerosol in two different periods (during wildfire and post-fire) in Los Angeles	(Verma et al. 2009)
	Activity correlated with WSOC content of DEPs	DEPs collected from late model HDDVs	(Biswas, Verma et al. 2009)
	Higher activity for SOA compared to POA. Activity negatively correlated with PAHs and positively correlated organic acids	Ambient ultrafine aerosol in two different periods (morning and afternoon period) in Los Angeles	(Verma et al. 2009)
	Increase in activity for the aged DEPs compared to fresh emissions.	DEPs	(Li et al. 2009)
	A major fraction of DTT activity was found to be contributed by SVOCs.	Ambient ultrafine aerosol (in Los Angeles) collected upstream and downstream of a thermodenuder	(Verma, Shafer et al. 2010)
	Activity correlated WSOC, WISOC, and OC content of PM	Gasoline, Diesel, and Biodiesel Cars (Euro standards)	(Cheung, Polidori et al. 2009)
	PAHs and hopanes, Zn, P, Ca (lube oil components)	Gasoline, Diesel, and Biodiesel Cars (Euro standards)	(Cheung, Ntziachristos et al. 2010)
	Activity correlated with OC	Ambinet aerosol (coarse, fine and UF) Los Angeles-Long Beach Harbor	(Hu, Polidori et al. 2008)
DHBA Assay	Activity was correlated with Cu and Fe, but the contribution of Cu was much higher compared to Fe.	Ambient ultrafine aerosol and DEPs (from newer HDDVs)	(DiStefano, Eiguren-Fernandez et al. 2009)
GAPDH Assay	Activity mostly associated with quinone and quinone like substances.	Ambient aerosol and DEPs	(Shinyashiki, Eiguren-Fernandez et al. 2009)

These assays have significant limitations to overcome for field use, including reaction times, even with added catalysts. These drawbacks make the use of such methods in the development of a field instrument challenging. Reliance on extraction of particulate matter from filters or liquid slurries of concentrated particles and subsequent handling of that extract is both time intensive and laborious. At present the DTT method is being used in the development of an online instrument, in which a PILS is coupled to a 'lab on a chip' microfluidic device that conducts the DTT reaction (Sameenoi, Koehler et al. 2012). This device reduces the reaction time typically used for the DTT assay by only measuring one point out of the usual five to determine the rate of DTT consumption, allowing for a 3 minute time resolution for sampling.

2.3.3 Nonreactive species generating ROS within cells (ROS activity)

Quantifying the increase of ROS levels within cells is perhaps one of the closest actual measurements of interest amongst all of the existing methods or surrogate assessments. The macrophage ROS assay (Landreman, Shafer et al. 2008) uses components that simulate the actual exposure and impact as closely as possible. PM2.5 filter samples are collected, over a period of 24 hours, similar to the federal reference method, divided in half and each extracted in deionized water. One extract is introduced into a buffered solution of rat alveolar macrophages. Alveolar macrophages, in rats and humans, are cells residing on the inner epithelial surface with direct exposure to inhaled particulate matter. They signal pulmonary inflammation, which is a strong indicator of PM toxicity, and have been shown to respond more uniformly and predictably than other cell lines. These cells are incubated at body temperature for two hours, at which point the

fluorescent ambient ROS probe (DCFHDA) is introduced to the cells. DCFHDA does not require deacetylation in a cellular environment as the acetates will be removed naturally within the cell. Using a microplate fluorescent reader, the fluorescent intensity is measured over 150 minutes. In addition to the direct assessment of the macrophages, controls and cell viability are also assessed. This particular method has been shown to be effective without requiring PM concentration; in fact, it was viable with Denver samples at less than 100 μg PM. Research has further shown that filter storage at 4C versus immediate extraction and analysis did not reduce reactivity, allowing for other studies to ship filters to groups with the technical capabilities of conducting the assay (Landreman, Shafer et al. 2008).

Several studies have used the macrophage ROS assay to compare results with other aerosol trends and PM speciation, as are detailed below in Table 2.3.3-1.

Table 2.3.3-1. Summary of macrophage assay findings.

Method	Major Findings	Source of Particles	References
Macrophage ROS Assay	Activity correlated with transition metals (V, Cr, Fe, Ni)	Ambient fine (<2.5 um) aerosol in two different periods (during wildfire and post-fire)in Los Angeles	(Verma et al. 2009)
	Activity correlated with OC and Vanadium	Ambient aerosol (coarse, fine and UF) Los Angeles-Long Beach Harbor	(Hu, Polidori et al. 2008)
	Activity correlated with transition metals (V, Ni and Cd)	Ambient ultrafine aerosol in two different periods (morning and afternoon period) in Los Angeles	(Verma et al. 2009)
	Activity correlated with Fe, Cr and Co content of DEPs. Chelation of metals substantially reduced the activity.	DEPs from newer HDDVs	(Verma, Shafer et al. 2010)
	Activity correlated with Fe, dust and WSOC sources in ambient atmosphere.	Ambient fine aerosol in Denver	(Zhang, Schauer et al. 2008)
	Activity correlated with transition metals (Mn, Co, Fe, Ni); highest correlation with Fe. Chelation of metals substantially reduced activity.	Ambient aerosol (PM10 and PM2.5) in Lahore, Pakistan	(von Schneidemesser, Stone et al. 2010)
	Activity correlated with soluble Fe content of PM	Gasoline Diesel and biodiesel cars (European standards)	(Cheung, Ntziachristos et al. 2010)

The macrophage ROS assay is a novel approach to using biological components with aerosol collection extracts to make a direct connection between exposure and impact within cells, but given the extent to which it requires biological controls and lengthy incubation times to assess the effects on the cells, it is not well suited for use in the field. It is not a great improvement in terms of reaction time over the traditional implementation of oxidative potential assays, given the preparation time and incubations alone for the base materials and the additional biological assays on the cell lines, regardless of their ease of maintenance. The stated reaction time for DCFHDA is long, likely a result of the absence of the typical catalyst, horseradish peroxidase, which might cloud results.

CHAPTER 3

OFFLINE CALIBRATION AND SENSITIVITY ANALYSIS

The probe 2',7' dichlorofluorescin (DCFH) was chosen as the most appropriate and comprehensive ROS detector for the purposes of developing an online gas and particle analytical instrument capable of measuring ROS associated with ambient fine particles. Of the ROS probes commercially available, DCFH had a long and well-documented record of sensitivity in both cellular and atmospheric aerosol applications (Black and Brandt 1974; Cathcart, Schwiers et al. 1983; LeBel, Ischiropolous et al. 1992; Hung and Wang 2001; Venkatachari, Hopke et al. 2005; Liu, Wu et al. 2007; Venkatachari, Hopke et al. 2007; Venkatachari and Hopke 2008; Wang, Hopke et al. 2011). Lack of specificity made DCFH attractive for a comprehensive ambient ROS measurement as opposed to a particular organic hydroperoxide or simply hydrogen peroxide. Its visible excitation wavelength further reduced costs for analytical equipment.

The primary goals of the offline analyses of the DCFH probe were:

- to verify DCFH suitability at the laboratory stage for making ROS measurements in solution,
- to evaluate some of the parameters to which DCFH had been reported sensitive (Black and Brandt 1974; Cathcart, Schwiers et al. 1983) with special attention paid to those that would potentially impact a continuous analysis setup the most.

3.1 Materials

DCFHDA was purchased from both Sigma Aldrich and Calbiochem (EMD Chemicals), depending on availability. Horseradish peroxidase (HRP) was purchased exclusively from Sigma Aldrich. Hydrogen peroxide (30%, w/w) was purchased from JT Baker via VWR.

Primary analytical equipment included a spectrofluorometer (Maya2000Pro, Ocean Optics, Dunedin, Florida, USA) with cutoff and longpass filters for wavelengths greater than 515 nm and a 200 μm slit. The spectrometer was further equipped with a flow-through cuvette cell of 450 μL volume with a light path of 10 x 4 mm (FIA-SMA-FL-ULT, . The excitation source initially used was a blue LED source manufactured by Mikropack (Ocean Optics, LS-475) exciting at 475 nm, though this was eventually replaced with a Jasco-manufactured 470 nm wavelength LED with adjustable voltage (LLS-470, Ocean Optics) to account for LED intensity loss with bulb age. Fiberoptic cables (SMA-905, Ocean Optics) completed the primary analytical apparatus.

Solutions were pumped through the flow through cuvette cell using an 8-channel peristaltic pump (Ismatec, .Opfikon, Switzerland). Any tubing, glassware or other vessels for working solution storage or transport were shielded in aluminum foil.

3.2 Reagent preparation

According to previously published methods (LeBel, Ischiropolous et al. 1992; Cohn, Simon et al. 2008) 2',7' difluorodihydrochlorofluorescin diacetate (DCFHDA) was dissolved in HPLC grade ethanol in a portable darkroom (Silver Edition HydroHut, Flora Hydroponics, Atlanta, Georgia, USA), and either used immediately or stored in the

freezer in an amber bottle, wrapped in Parafilm to prevent evaporation of the solvent. To prepare the working solution of some concentration of DCFH, 0.01 N NaOH was added to the DCFHDA solution to remove the acetates. After thirty minutes, the solution was buffered with a sodium phosphate buffer (pH 7.4) to halt the reaction, dilute the working reagents and bring the pH of the working solution to 7.2 (allowable range, 7.2 – 7.4). pH was verified with a handheld pH monitor (VWR). HRP (Type II, Sigma Aldrich) was then added to the solution to bring it to 0.5 – 1 units HRP/mL solution. The working solution (DCFH and HRP) was then stored in an amber vessel or foil-wrapped flask in the laboratory refrigerator at 2 ° C and discarded after a period of 2 days, or longer during the assessment of DCFH auto-oxidation discussed below. The original standard working solution was 5 μM DCFH with 0.5 units/mL HRP. A detailed description of these reagents and the final method by which they are created and combined can be found in Appendix A.

3.3 Offline sensitivity testing

The initial evaluation of DCFH was conducted following the method described by Hung and Wang (Hung and Wang 2001) in which the probe was used to quantify the ROS concentrations from ambient particle filter extracts.. 3 mL of DCFH-HRP solution were pipetted in the darkroom into amber vials, which were then covered with predrilled caps (1/16” diameter) and sealed with paper laboratory tape. These vials were stored in the refrigerator until use.

For analysis, the tape was briefly removed from the vials and 0.1 mL of either deionized water (dI) or a hydrogen peroxide standard was pipetted through the cap hole .

The tape was replaced and the vial briefly inverted to ensure that no peroxide remained uncombined with the DCFH solution. Per the method described by Hung and Wang, again, the vials were allowed to incubate in a 37 ° C water bath, made from a hot plate, jar or baking dish of tap water and a thermocouple to measure the temperature, for fifteen minutes. The solution was then briefly agitated and placed in line with the analytical system, shown below in Figure 3.3-1. A peristaltic pump moves the DCFH-HRP-H_2O_2 solution at 0.4 mL/min through the flow through cell, while a selector valve allows for dI to be pumped when not measuring DCFH intensity. A small glass debubbler was also employed to reduce the signal interference by small air bubbles that may be introduced into the system, also run from the peristaltic pump at approximately 10% of the overall sample flow. Sufficient dI was allowed to move through the system to return the fluorescent signal to a baseline value before analyzing the next sample. The entire system was plumbed with green PEEK tubing (1/16" outer diameter, 0.030" inner diameter, Upchurch Scientific, Oak Harbor, Washington, USA).

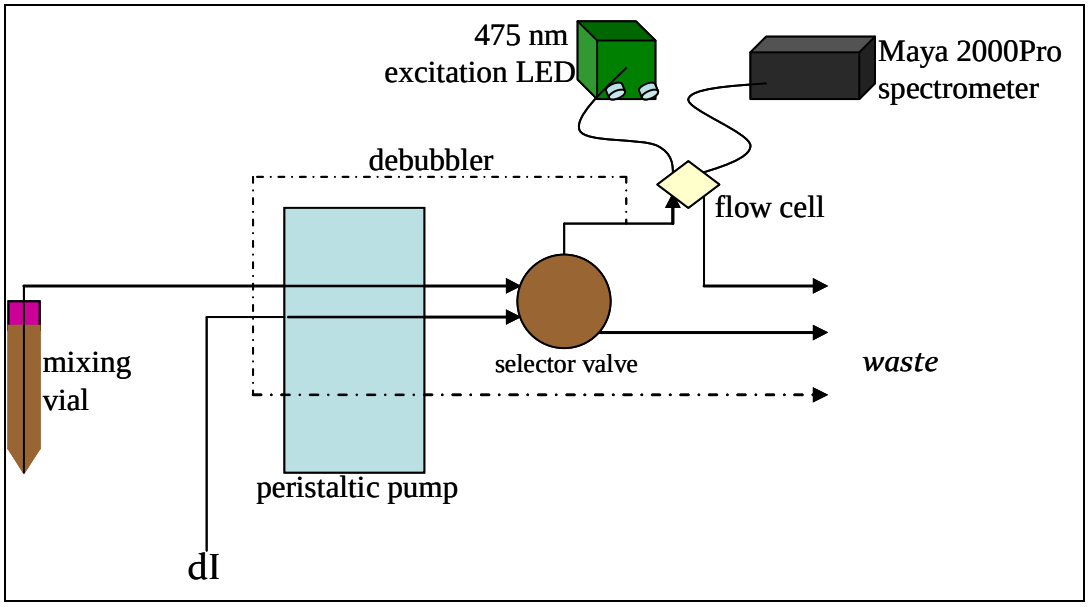

Figure 3.3-1: Basic vial schematic for offline ROS analysis

As the solution moves through the flow cell, it is excited by the 475 nm light source, which causes the DCF* to fluoresce at 530 nm. This light intensity is transmitted via the fiberoptic cable to the Maya2000Pro. Fluorescent intensity was measured using SpectraSuite from Ocean Optics. Signals were generally recorded of the fluorescent signal at 530 nm, with an integration time of 500 msec and average of 10 scans. A dark spectrum was determined by blocking all light from the spectrometer sensor and measuring the residual intensity. This was subtracted from the light spectrum via SpectraSuite. Intensity values reported are average intensities of measurements made once the fluorescent signal was stabilized, after a minimum of ten minutes from powering on the light source. Pure dI also provides a measureable signal at 530 over the dark measurement, which is subtracted out with the blank corrections and also provides a useful measure of light source intensity over time.

An example of an initial calibration using final solution concentrations H_2O_2 of 100-400 nM is shown below in Figure 3.3-2. This sample range was chosen as a representative span for the concentrations reported in ROS particle analysis from filter measurements (Hung and Wang 2001; Venkatachari, Hopke et al. 2005; Venkatachari, Hopke et al. 2007).

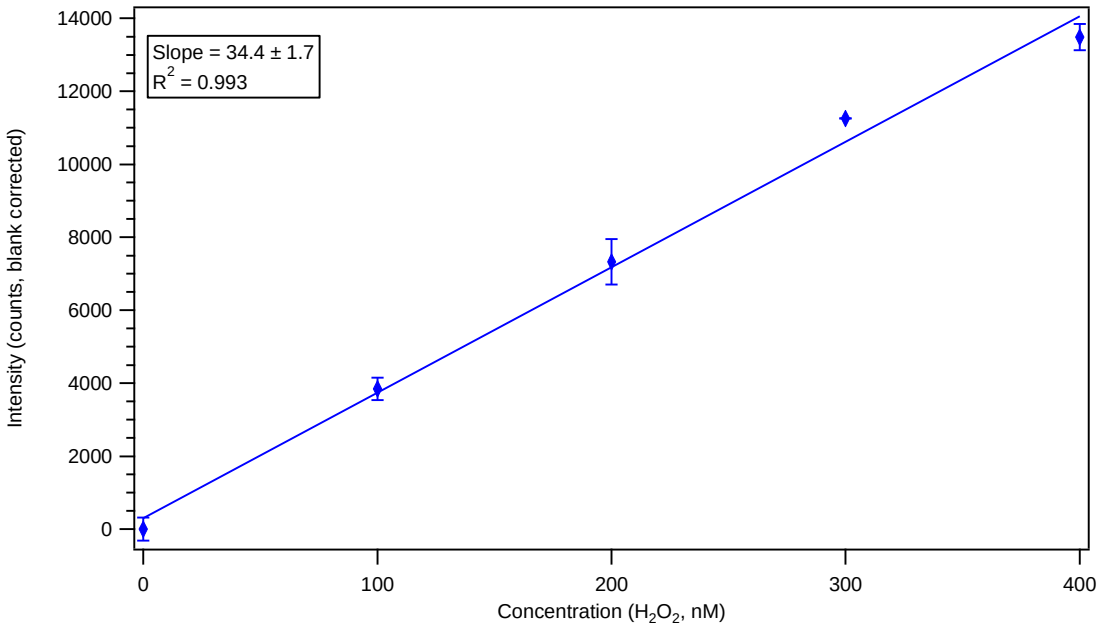

Figure 3.3-2: Initial calibration of offline ROS assay using DCFH. Error bars represent the standard deviation of the measurements made at a given concentration (n = 5)

3.4 Sensitivity analysis

Previous work has reported the need to control the working solution storage temperature, storage time (working solution age), pH, and other reaction parameters including reaction temperature, pH and reaction time to achieve maximum reaction of DCFH with peroxides. These parameters should also be optimized to reduce

autooxidation during storage and use of the working solution (Black and Brandt 1974; Cathcart, Schwiers et al. 1983). The following section investigates variables known to affect DCFH performance, which will then guide the development on the online instrument.

3.4.1 DCFH age

DCFH is prone to auto-oxidation when in solution (LeBel, Ischiropolous et al. 1992; Rota, Chignell et al. 1999; Jakubowski and Bartosz 2000; Afzal, Matsugo et al. 2003; Wardman 2008), which is a major drawback to its use as a probe during extended field studies. The required use of HRP is also problematic as the enzyme has been reported to react directly with DCFH to produce DCF without the presence of ROS (Towne, Will et al. 2004; Veitch 2004). As the solution ages, the blank values of the solution increase, as an ever-growing percentage of DCFH has reacted prior to exposure to peroxides. This subsequently reduces its sensitivity to peroxides, resulting in a reduced calibration slope over time. Since a field instrument would not likely have the capability to keep working reagents at a low temperature to reduce auto-oxidation and other potential chemical degradations, determining the useful lifetime is critical to effective and consistent operation in the field.

Figure 3.4.1-1 show a comparison of two different batches of DCFH-HRP working solution, assessed over a period of time to assess the influence of aging. In all cases, the working solution was kept in a refrigerator at 4° C between measurements, which was expected to reduce the effect of aging to some extent.

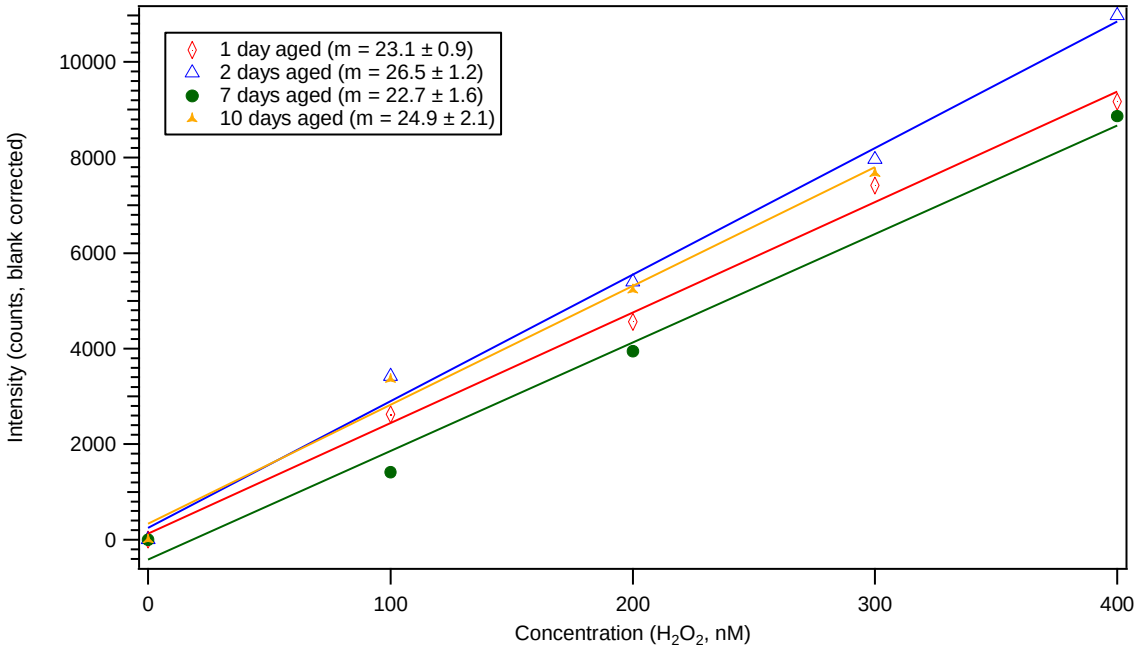

Figure 3.4.1-1: DCFH response sensitivity over time

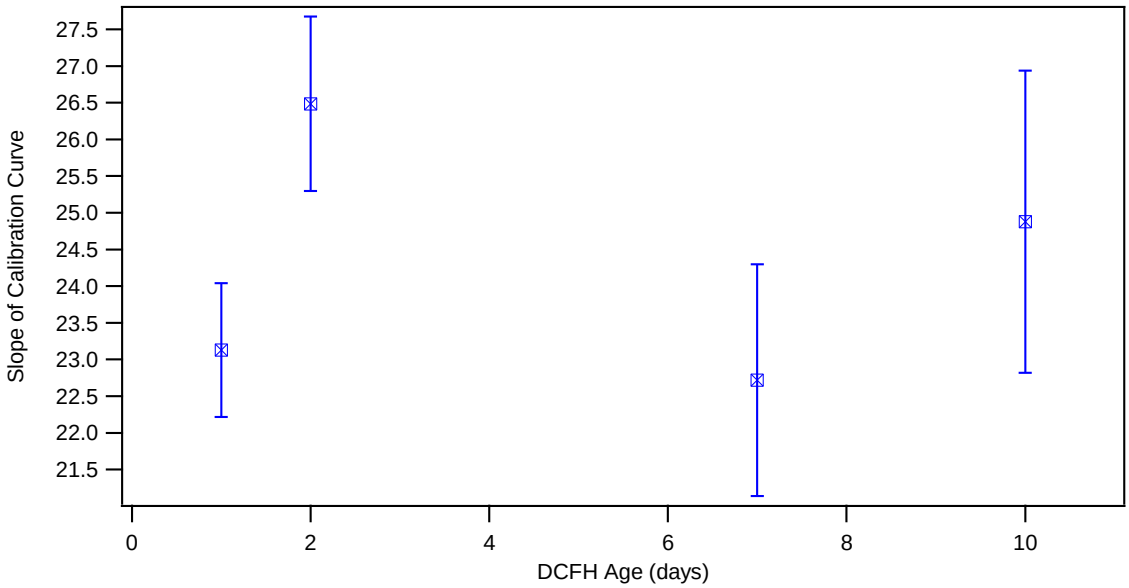

Figure 3.4.1-2: Slope comparison for aged DCFH

From the offline analyses, we concluded that DCFH solutions may be viable to a period of ten days or more, with the caveat of cold storage. DCFH stored regularly at ambient temperature was not assessed until well into the online instrument development phase, and then, only in terms of blank measurements.

It should be noted that the ROS calibration standard, hydrogen peroxide, is itself an unstable compound. Standards were made from serial dilutions from stock hydrogen peroxide (30% w/w). Final standards and their proximate serial dilutions were stored in 15 mL amber Nalgene centrifuge tubes (Nalgene or VWR brand, VWR) or for larger volumes, amber Nalgene bottles in the refrigerator and discarded after a maximum of 7 days. When low intensity results could not be attributed to an error in DCFH working solution makeup, DCFHDA viability or in standard storage, the stock hydrogen peroxide was discarded and a new bottle was purchased, typically on the order of 9-12 months.

3.4.2 Reaction temperature

Several papers report conducting the DCFH-HRP analysis, either intracellularly or for filter extraction at 37° C (Cathcart, Schwiers et al. 1983; Hung and Wang 2001). This temperature is the ideal temperature for performance of HRP as well as the average temperature of the human body. Temperature for the offline reaction was studied through use of the incubation temperature of the water bath, as shown in Figure 3.4.2-1 below.

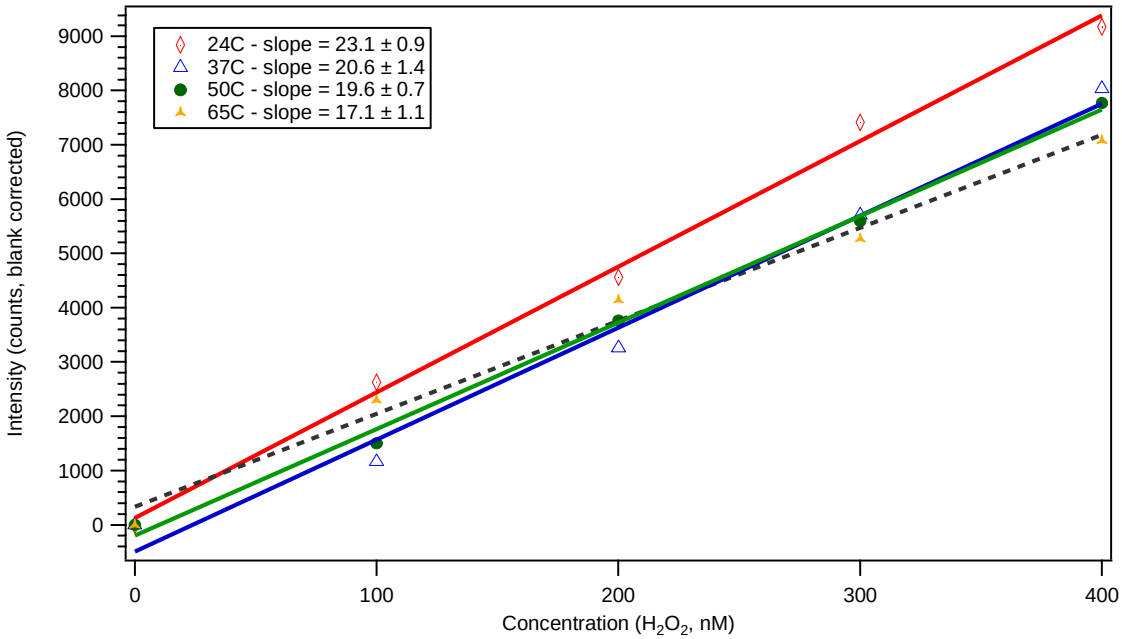

Figure 3.4.2-1: Variation of DCFH response with temperature.

The largest slope found in this set of experiments was that for the ambient (24C) sample set. This value is significantly higher than that of the slope for the 37C set and that of the 50C set, which are not significantly different from each other. The 65C set is significantly lower than all three of the previous temperatures evaluated, suggesting that some enzyme denaturation occurs at sufficiently high temperatures, and the reaction is less catalyzed due to this loss. These experiments suggest that no temperature increase over typical indoor ambient values would be necessary, indicating that heating elements would not be required in further development of an instrument.

3.4.3 DCFH concentration

Ambient particle phase studies (Hung and Wang 2001; Venkatachari, Hopke et al. 2007) cited using a concentration of DCFH in the working solution of 1 µM. A more recent online study (Wang, Hopke et al. 2011) indicated the use of a 5 µM DCFH solution. Higher concentrations of DCFH in the working solution could lead to increased auto-oxidation while also increasing sensitivity vis a vis the calibration slope. This was considered to be a variable of some importance for an online system, where higher concentrations could reduce reaction time. Below in Figure 3.4.3-1, the calibration slope of a 10 µM solution is compared to the slope of a 5 µM solution of DCFH. (The concentration of HRP was increased to 1.0 units/mL for the 10µM solution.)

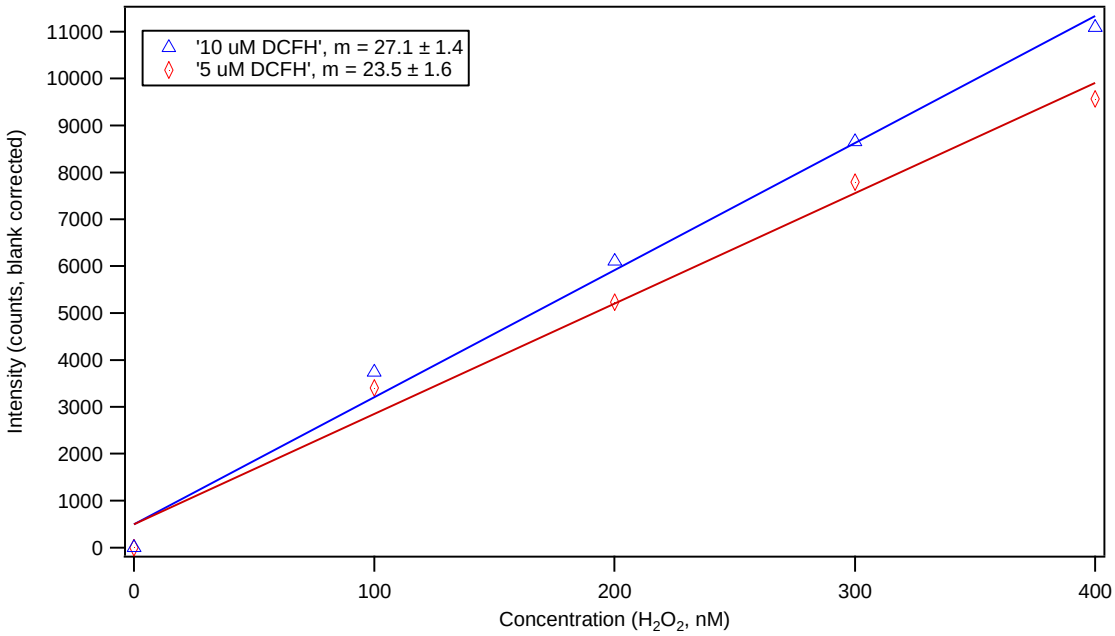

Figure 3.4.3-1: Variation of DCFH sensitivity to working solution concentration

From Figure 3.4.3-1, the 10 μM DCFH working solution had a significant improvement in value over that of the 5 μM solution. This set of tests was the deciding factor in working from this point on with concentrations of 10 μM DCFH for other tests and for the online analyses.

3.4.4 Reactant:sample volumetric ratio

In vitro experiments allow for a significant excess of reactant (DCFH) to sample (H_2O_2) both in terms of volume and moles. A continuous online analytical system was unlikely to allow for a 30:1 volumetric ratio of DCFH:H_2O_2 since combining such disparate flows presented challenges from an effective mixing perspective. To evaluate this parameter, a reduced volume of DCFH working solution was pipetted into a series of vials, from the initial 30:1 volumetric ratio (3 mL of DCFH solution to 0.1 mL hydrogen peroxide standard) down to 9:1, or 0.9 mL DCFH solution for 0.1 mL of H_2O_2 standard, the concentrations of which were decreased to maintain a consistent final H_2O_2 concentration. Figure 3.4.4-1 below is an example of the variability in intensity at a final standard concentration of 300 nM H_2O_2 with a varying volumetric ratio of reagent to sample.

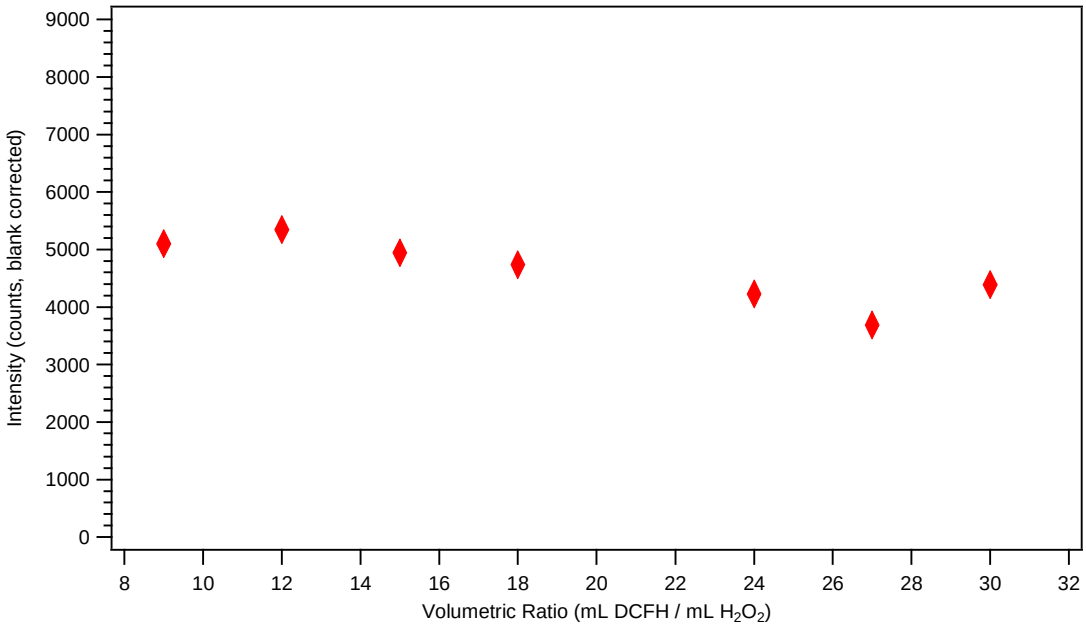

Figure 3.4.4-1: Variation of DCFH sensitivity to a reduced volumetric ratio

The standard deviation of the samples from Figure 3.4.4-1 was 570 counts (raw fluorescent intensity at 530 nm). The standard deviation of repeated trials for a single concentration ratio (the initial volumetric ratio of 30:1) averaged around 300 counts. These experiments do not show a trend for decreasing intensity as the volumetric ratio is decreased. This indicates that a lower ratio, in a batch or offline setting, would be feasible for future use. This may be due to the long incubation time of typical offline analyses and thus the ability for the full volume of sample to react with all available DCFH.

3.4.5 Reaction time

The time for the reaction to near completion is a critical component for the development of an online system. While offline studies have traditionally incubated

samples for 15 minutes (LeBel, Ischiropolous et al. 1992; Hung and Wang 2001; Venkatachari, Hopke et al. 2005; Venkatachari, Hopke et al. 2007; Venkatachari and Hopke 2008), the reaction may be mostly complete in less time. A faster reaction would increase the sampling rate in the eventual online instrument. In these tests, 0.1 mL of hydrogen peroxide standard or dI were pipetted into the vials as described previously with 3 mL of DCFH solution, briefly inverted to ensure that all liquids were combined and immediately placed in line with the detector. The sample line from vial to detector was shortened as much as possible to reduce the delay time from combination of DCFH and peroxide to initial detection of fluorescence, using the same 0.030" ID PEEK tubing as in the standard flow analysis setup from Figure 3.3-1. The residence time prior to detection was 30 seconds. Figure 3.4.5-1 below is an example of the time series of one such test, in which standards for 200 nM and 300 nM H_2O_2 were evaluated as well as a blank, i.e. dI instead of a standard.

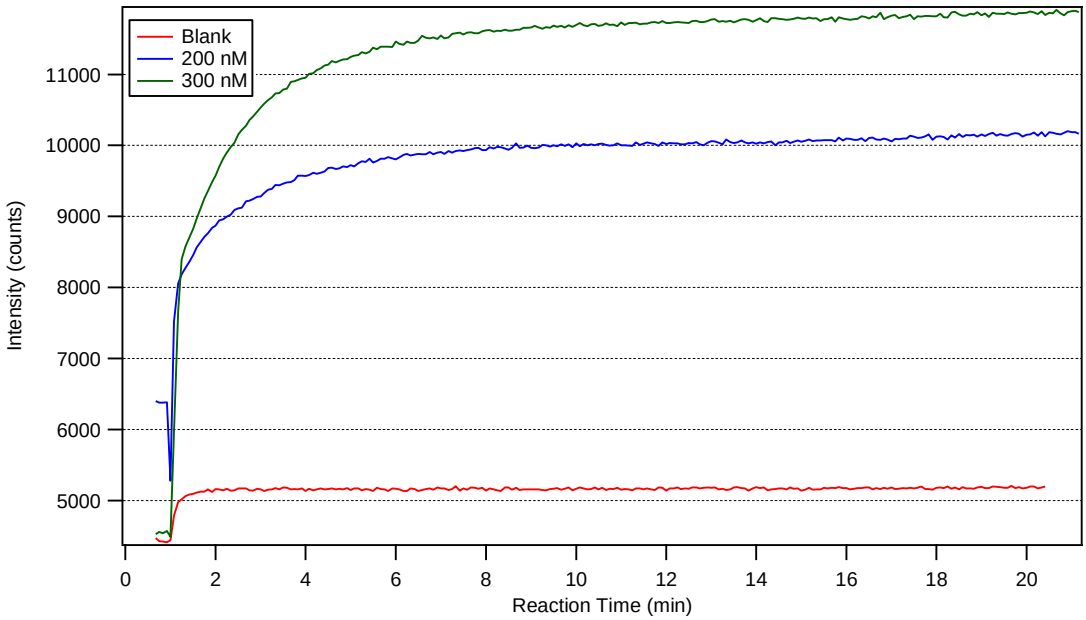

Figure 3.4.5-1: Reaction time series of DCFH.

The curves in Figure 3.4.5-1 represent the reaction progress of DCFH with either dI or the indicated standard concentration. Intensity increases as more of the eventual total of DCFH reacts with the available peroxide until there is a leveling off to the slow auto-oxidation level of fluorescent intensity increase (not readily apparently on this scale). After approximately 6.5 minutes, the reaction for the standards can be seen to be proceeding at this rate of what can be considered completion. At this time, the 200 nM standard has reached 97.4% of the intensity measured after 20 minutes, whereas the 300 nM standard has reached 96.7%. The blank values level off very rapidly, prior to 2 minutes, as lower concentrations are expected to reach a shorter completion time than higher ones. In fact, for each standard to reach 90% completion, where the intensity of completion is taken to mean the intensity achieved for that specific standard concentration after 20 minutes, these intensities are reached at 2.7 minutes for the 200 nM concentration and 3.5 minutes for the 300 nM concentration.. These times indicate a minimum amount of time for the reaction to proceed in an online setting, much less than the times used previously for offline assessments.

3.4.6 Parameters not evaluated

Early assessments of aqueous hydrogen peroxide in a laboratory setting using DCFH (Black and Brandt 1974) evaluated the effect of solution pH on the apparent fluorescence of DCFH, demonstrating a rapid increase in fluorescence for pHs between 4.0 and approximately 7.0, with a lack of additional response between pHs of 7.0 and 10.0. Using the sodium phosphate buffer as the basis for the working solution maintains a pH between 7.2 and 7.4, which is also a necessary parameter for HRP activity as well.

While pH was routinely monitored in new solutions and as the solution aged during the initial efforts to create a working fluorescent probe, it was not varied during these analyses. DCFH as a general ROS probe has also been evaluated against other ROS such as t-butyl-hydroperoxide (TBHP) (Cathcart, Schwiers et al. 1983). Without more complex ROS generation capabilities on hand, hydrogen peroxide was used as a surrogate for all evaluations.

3.5 Conclusions from offline analyses

The set of experiments described in this chapter helped determine the parameters under which an online instrument for the measurement of ROS in the atmosphere would be developed. A summary of these conclusions are shown below in Table 3.5-1, which were then the parameters maintained in the further development of the instrument. The reagent and sample mixtures were not heated and the working solution remade after two days and at a concentration of 10 mM with 1 unit/mL of HRP. The mixing ratio of the volume of reagent to the volume of sample was not decreased below 9:1, and at least three minutes were allowed before taking measurements of intensity for conversion into concentrations after the sample and working solution were mixed.

Table 3.5-1: Parameters suggested by offline analyses for use in online instrumentation

Parameter	**Value**
Maximum DCFH age	2 days
Reaction temperature	ambient
DCFH concentration	10 μM
Volumetric ratio	Arbitrary (9:1 – 30:1)
Minimum reaction time	3 minutes

CHAPTER 4

ONLINE INSTRUMENT DEVELOPMENT: SENSITIVITY ANALYSIS AND FIELD MEASUREMENTS

Once the in vitro chemistry and its variables were understood and controllable, the basic analytical system was adapted into an instrument that included a collection apparatus for ambient ROS and equipment for automating the analysis. The completed system was initially deployed for testing at the Jefferson Street SEARCH site during February 2012. The instrument was then deployed during the first phase of Project 1 of the Southern Center for Air Pollution and Epidemiology (SCAPE) in and around the Atlanta area during the summer of 2012.

4.1 Particle collection options

The collection phase of an online instrument is as important as the analytical portion. In attempting to measure ROS in the particle phase, it is necessary to exclude the gases, levels of which are thought to exceed particle concentrations by 1-2 orders of magnitude. Three general approaches were available: using a collection device such as a PILS that would not include the gas phase by the nature of its collection method, or using a method such as a mist chamber that would collect both and either a) removing the gas phase prior to the chamber via denuders or b) measuring the total ROS (gas + particle) and subtracting from it the subsequently measured ROS(gas) concentration, determined by sampling through a particle filter. An instrument using the PILS for ROS(p) collection has already been developed (Venkatachari and Hopke 2008) and tested (Wang,

Hopke et al. 2011) by one research group, as was briefly described in Section 2.3.1. Some preliminary work was done to operate a similar instrument, which ultimately did not prove fruitful. This work and its preliminary findings are described in Appendix B.

4.2 Mist chamber

Originally known as the Cofer scrubber, mist chambers have been developed to collect water soluble gases and particle for online analysis. (Cofer III, Collins et al. 1985; Cofer III and Edahl 1986; Spaulding, Talbot et al. 2002; Anderson, Dibb et al. 2008). Briefly, the mist chamber is a cylindrical glass structure with an inlet at the bottom for air flow, a port on the side for introduction and removal of liquids, and a nebulizing nozzle. The latter consists of a nozzle and capillary running from above the nozzle to the liquid reservoir at the bottom of the chamber. Some minimum volume of liquid, usually water, is placed inside the mist chamber. Venturi forces created by the airflow accelerated through the nozzle, draw liquid from the reservoir into the air jet and creating a spray which then refluxes down the sides of the chamber. A hydrophobic filter situated at the top prevents loss of liquid and water soluble atmospheric constituents while allowing air out. The liquid is continually recycled through the chamber, into which the soluble compounds from the airstream are entrained. Sample air flow is stopped after a given interval, at which point the liquid and soluble components are withdrawn from the chamber for analysis. Analysis of the sample can occur while the next sample collection cycle proceeds. Figure 4.2-1 shows a general schematic of the mist chamber, while Figure 4.2-2 shows design documents as provided by Dr. Jack Dibb, University of New Hampshire.

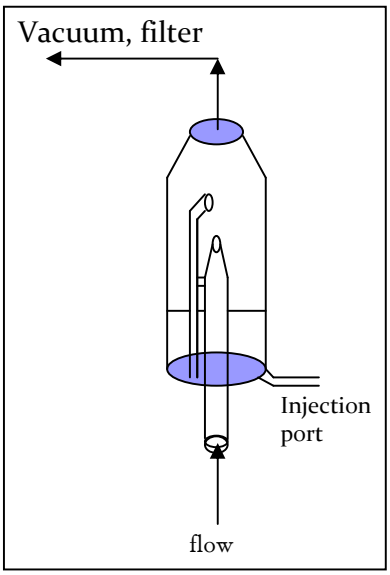

Figure 4.2-1. Mist chamber design.

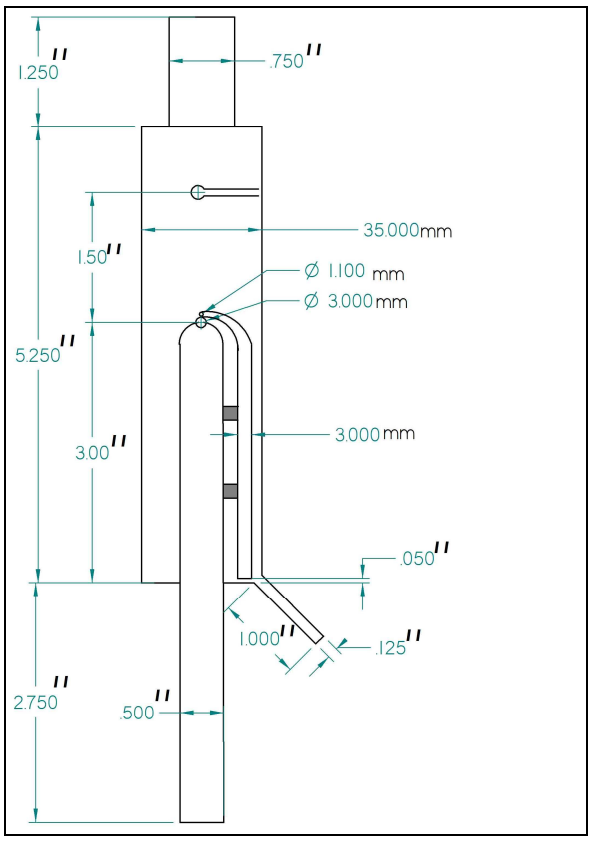

Figure 4.2-2. Design schematic of mist chamber from the University of New Hampshire

Major benefits of the mist chamber include operation without heating the sample, and the ability to select from a range of integration times so samples can be concentrated. At ambient temperature, hydrogen peroxide is expected to partition to the liquid phase at a rate of 99.5% based on its Henry's Law constant (K_H) constant, an indicator of the amount of a compound that will dissolve into a solvent at a given temperature. The mist chamber has been shown to effectively collect compounds with a K_H of over 10^3 L-atm/mol (Spaulding, Talbot et al. 2002) The potential drawbacks of the system include the need for a batch operation process to collect and analyze ROS. This system can be considered non-ideal in the interests of collecting as many samples as possible over as short a timeframe as possible, i.e., achieving a continuous monitoring system. However, sampling in batches could allow for necessary collection of sufficient particle mass in the event that concentrations are under the limit of detection. The mist chamber will also use more dI than an instrument such as the PILS. Without an effective gas removal system, the inclusion of soluble gases during particle collection could be a problem when focusing solely on the particle phase.

4.2.1 Mist chamber collection system setup

The overall setup of the mist chamber instrument is shown in Figure 4.2.1-1 and includes the following elements. The sample air inlet at the bottom of the mist chamber is connected to an automatic valve that either directs airflow through a 47 mm filter pack (URG, Carrboro, North Carolina, USA) containing a 2.0 μm pore size Teflon filter (Zefluor, Pall Corporation) for measurements of only soluble gases, or bypasses this filter to measure all soluble gas and particle components. Typically a copper sample line runs

outside to a $PM_{2.5}$ cyclone (16.7 lpm for cut size of $PM_{2.5}$, URG). To reflux the liquid spay generated in the mist chamber, another 47 mm filter pack (URG) was fitted to the top of the chamber and contained a 1.0 μm pore size hydrophobic filter (TefSep, Pall Corporation). This filter eventually became loaded with insoluble particle mass, resulting in a reduced sample flow rate and so was changed every 3-4 days, depending on the mass loading of the ambient air. Following the refluxing filter, sample air passed through a water trap and a mass flow controller (GFC-47, Aalborg), set a given flow rate of typically 20 lpm, and finally through a vacuum pump (carbon vane, Gast ¼ hp,).

A Kloehn syringe pump (V6, 48K resolution, part number 55022) equipped with an 8-port valve and 10 mL syringe provided automatic liquid delivery to and from the mist chamber. One port is connected to the liquid inlet of the mist chamber using Pharmed tubing and PEEK threaded fittings. The other ports led to a reservoir of the DCFH-HRP working solution, a dI tank, a waste vessel, and a 15 mL amber mixing vial of the same type as was used for offline analyses, also equipped with a predrilled cap. The remaining three ports could be used for up to two hydrogen peroxide standards for automatic calibrations and an open port for introduction of air as required. The V6 pump also controlled by means of I/O ports on a rear logic board the power to the Gast vacuum pump through a solid state relay, as well as the position of the valve directing air flow around or through the Teflon filter (ROS phase selection valve), and a two position liquid selector valve to change the source of the liquid flow into the fluorescence detection flow cell.

A 4-channel peristaltic pump (Ismatec) continuously moved liquid from either the 15 mL amber mixing vial or the dI reservoir through the flow cell, to which the light

source and the spectrometer were attached. This amber mixing vial contains two PEEK tubing lines inserted through the hole in the cap. The line from the peristaltic pump reaches to the bottom of this mixing vial while the line from the syringe pump valve extends only a short distance past the cap. This setup allows for all liquid to be withdrawn completely via the longest line from the mixing vial, while the shorter line does not reach the liquid at any point. A third channel on the peristaltic pump also controls flow from a glass debubbler of approximately 0.5 ml internal volume, in line just prior to the flow through cell. The fourth channel available on the pump removes any liquid from the water trap to protect the mass flow controller from liquid. The glass syringe and all other clear portions of this system are shielded from light with aluminum foil.

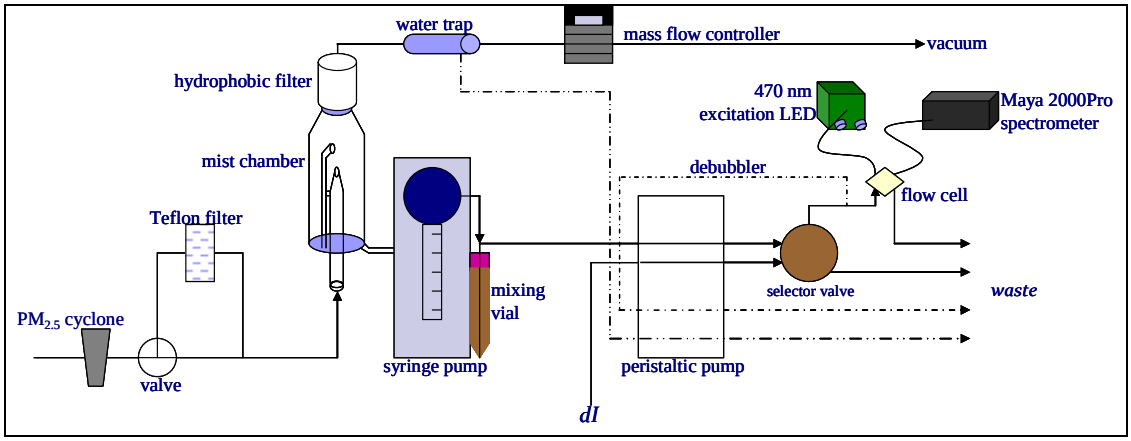

Figure 4.2.1-1: General mist chamber system schematic

This sampling system was designed for the high transport efficiencies of particles, not gases, since the focus is in measuring particle-phase ROS. Losses of gases may be substantial with this setup, which is advantageous to the implementation of a difference

method for determining particle ROS, though limits interpretation of the ROS(g) measurements.

4.2.2 General automation of mist chamber system

The following describes a typical sample collection and analysis cycle.

Analysis of Mist Chamber Sample:

Using a looping routine in the Kloehn Control software, the syringe pump injects between 10 and 30 mL of dI into the mist chamber for ambient sampling cycle. The Gast vacuum pump is started by the syringe pump and operated for a period of between 5 and 30 minutes to collect soluble ROS ambient species into the mist chamber collection liquid. The V6 pump then shuts off the vacuum pump and withdraws 1.5 mL of the ROS-laden solution from the mist chamber, then discarding 0.5 mL of this from the top of the syringe, in the event that any air that may have been introduced to the syringe. 9 mL of DCFH/HRP working solution are then added to the syringe. The combined total 10 mL of DCFH/HRP-particle solution is forced into the mixing vial. This process completely mixes the sample of dissolved ROS components and DCFH/HRP. During this period the peristaltic pump is pumping dI through the flow cell and generating a baseline of fluorescent intensity for the spectrometer to measure. The contents of the reaction vial are allowed to react for one minute while being pumped to the selector valve, after which the syringe pump changes the selector valve to direct the mixing vial solution into the flow cell.

Cleaning of Mist Chamber:

During the analysis of the ambient sample by the spectrometer, the syringe pump cleans the mist chamber prior to reloading it for another sample by draining and discarding the remaining sample liquid from the mist chamber. Deionized water is added to the mist chamber. The ROS phase selection valve is adjusted to filter the ambient air while the vacuum pump is operated for 30 seconds, allowing particle free air to reflux water down the top and sides of the chamber cleaning both the mist chamber and rinsing the syringe and sample lines for next cycle. This water is withdrawn and discarded.

After 2.5 minutes of analysis time by the spectrometer, the selector valve switches back to the dI line to rinse the flow cell while discarding the remaining sample solution. The syringe pump also withdraws the remaining DCFH solution from the mixing vial and discards it in order to empty the vial rapidly and restart the sampling cycle. The syringe pump then flushes the mixing vial by pushing 10 mL of dI to the vial and withdrawing the remaining liquid after 10 seconds, which allows some dI to clear out the sample lines of the peristaltic pump, and for the mixing vial to be rinsed between sampling runs.

Since part of the analysis time includes preparing the mist chamber for the next measurement, there is a delay of at least 5.5 minutes between sampling cycles. For example, one complete cycle of the general ROS sampling and analysis cycle took 10.5 minutes when collecting sample in the mist chamber for 5 minutes. Longer duty cycles were employed when the mist chamber sample collection time was increased to collect more concentrated samples.

The mist chamber used in this instrument was constructed by the department glass blower. There can be considerable variation between chambers and their operational

collection efficiency must be verified. Mist chamber collection efficiencies were determined by comparing the collection of sulfate with a simultaneous operation of the PILS-IC system. For this evaluation, the ROS instrument was operated entirely in ROS(tot) mode, without filtering the particles from the airflow. The collected liquid was drawn from the mist chamber into a vial, which was then analyzed by the same IC measuring the sample collected by the PILS. Multiple measurements of ambient $PM_{2.5}$ sulfate concentrations were conducted at different mist chamber sample air flow rates. The resulting collection efficiency graph of Figure 4.2.2-1 shows that this specific mist chamber should be operated at a minimum flow rate of 15 lpm,. While flow rates above the minimum would be valuable in collecting sufficient ROS to measure above the limit of detection., this particular setup was limited to approximately 25 lpm given the large pressure drop across various elements of the system, including the water trap and wetted hydrophobic reflux filter.

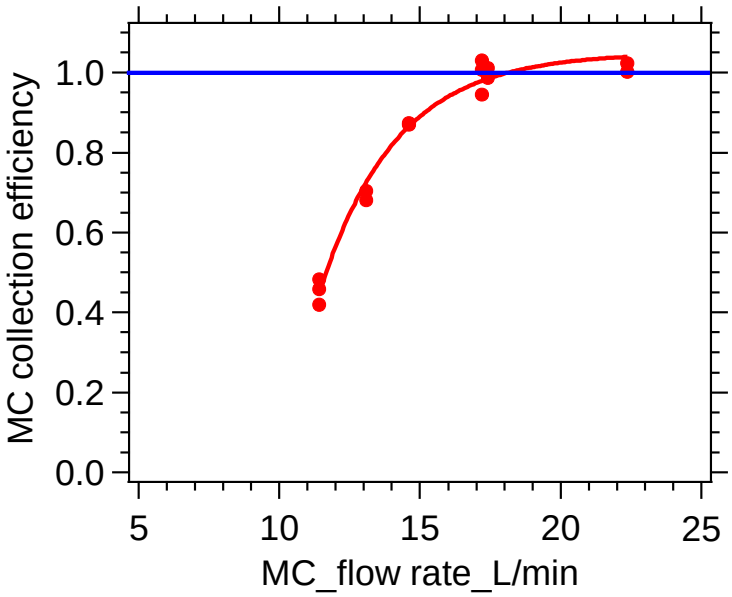

Figure 4.2.2-1. Mist chamber collection efficiency

4.2.3 Calibrating the online ROS instrument

The ROS instrument as described can be calibrated in an offline but automatic mode and verify standard concentrations as part of its routine operation. In its offline, non sampling mode, a similar Kloehn Control program is used to the standard automation. The mist chamber elements of the automation are removed, and instead of liquid from the mist chamber being combined with the DCFH working solution, the same volume of a standard is combined instead. "Blank", or auto-oxidation measurements, are made using dI instead of the standard, as they were in offline analyses. Figure 4.2.3-1 shows a typical calibration plot, using lower range standards as determined by the measured ambient concentrations.

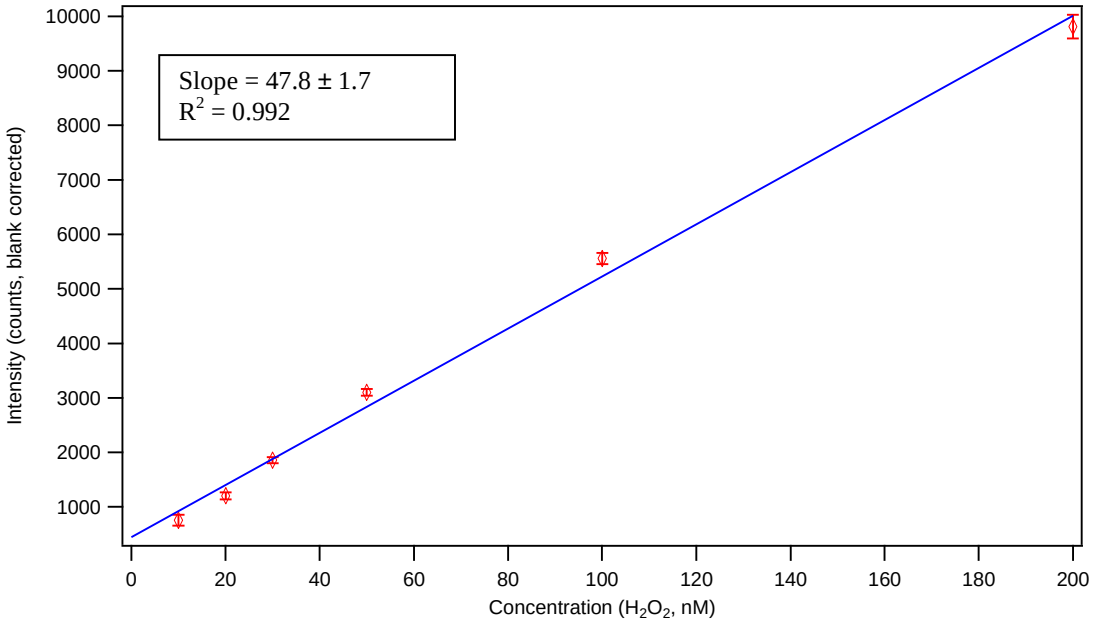

Figure 4.2.3-1: Mist chamber calibration plot.

As blank measurements are technically measurements of the auto-oxidation state of the DCFH working solution, allowing for the dynamic correction of the sample signal over time, they are conducted during the routine sampling operation periodically. The

"blank" signal is generally measured after every 6 ambient measurements, or nearly every hour. Figure 4.2.3-2 below shows a sample of the linear drift over a 48 hour period of the blank signal during field testing of the instrument.

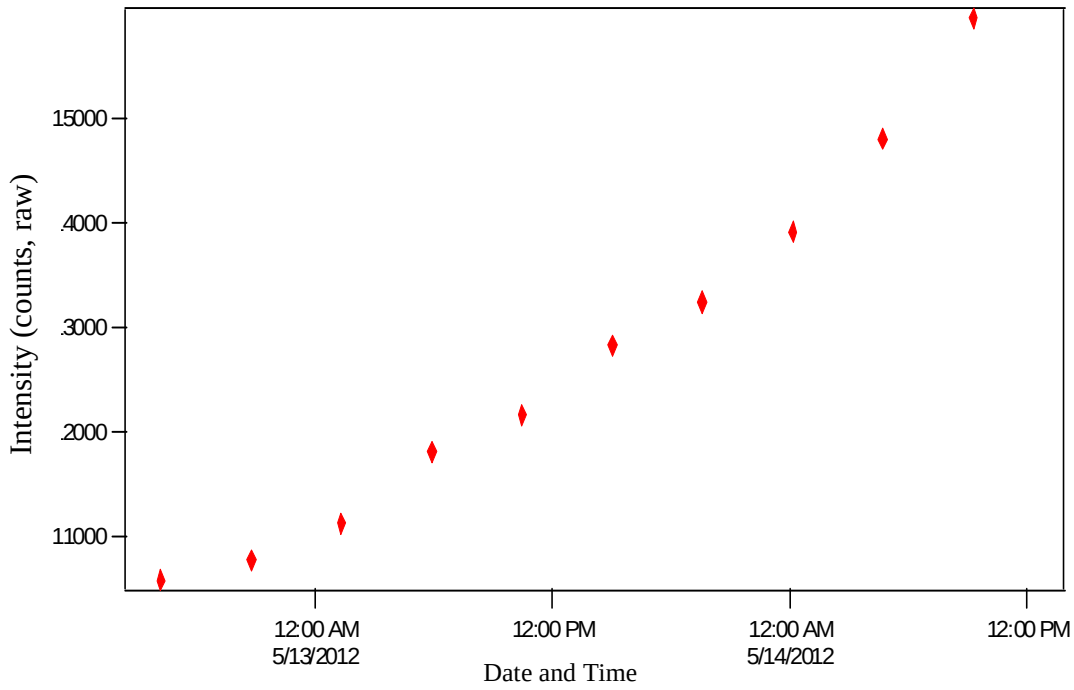

Figure 4.2.3-2: Auto-oxidation ("blank") measurements of DCFH over time, demonstrating the linear drift of the DCFH working solution

While the refluxing hydrophobic filter that retains liquid in the mist chamber is very effective, there will inevitably be some liquid loss related to ambient temperature, volume of liquid, relative humidity, air flow and operational sampling time. To account for this loss, the final volume of liquid retained by the mist chamber is measured periodically to account for the losses. This loss was also a motivating factor in the short sampling periods initially employed during the instrument's field deployment. There is

additional uncertainty in the liquid lost by the mist chamber since it is not possible to withdraw all liquid from vessel from the injection port – some will be retained along the filter and the mist chamber walls. This represents an uncertainty of ± 10% of the final liquid volume.

4.2.4 Calculation of ambient ROS concentration

Determination of the ROS concentration in the ambient air using the previously described method is calculated using the following:

$$C_a = \left(\frac{I-b}{a}\right)\left(\frac{V_s}{1000 Q_a t}\right)$$

Where

C_a = Concentration of ambient ROS in H_2O_2 equivalents (nmol ROS /L air)
I = Intensity of fluorescent signal (counts, relative)
b = slope intercept from calibration linear fit
a = slope from calibration linear fit
V_s = Final solution volume (mL) in mist chamber)
Q_a = Average air flow through mist chamber for one sampling period (lpm)
t = time sample drawn through mist chamber (min)

This value is reported in nmol ROS / m^3 air by multiplying *Ca* by 1000 L / m^3 air.

4.2.5 Limit of detection for system

The limit of detection for the instrument was determined by three times the standard deviation of the 'blank' measurements (working solution and dI) and converted to liquid or ambient concentration. 'Blank' measurements for this purpose were conducted offline so that there would be minimal auto-oxidation between each

measurement. The liquid concentration limit of detection for the system was calculated to be 0.28 nM H_2O_2 equivalents, or 0.029 nmol/m^3 for the typical operational values of the mist chamber instrument, in which the final liquid volume is 9.7 mL, the air flow rate is 20 lpm and the sample collection time is 5 minutes. The method by which a different LOD was employed for the particle calculations is discussed later.

4.2.6 Measurement precision

The precision of the measurements is determined by the standard deviation of repeated standards, a value that is most accurately determine in a calibration setting but also in the periodic measurement of standards during the routine operation of the instrument. The latter is a way in which to include any systemic variability that might affect the sample analysis during the cycling of the program. It also, however, includes more uncertainty since the standards need to be corrected for auto-oxidation using a linear interpolation of those measurements over time. Here, precision is reported based on variability in off-line calibrations.

Based on repeated calibration standards, the precision of this system is 1.26 nM (liquid concentration), or under normal operating parameters, 0.025 nmol H_2O_2 (equivalents) /m^3 air.

4.3 Mist chamber system refinements

Multiple components of the system as described above did not exist in the initial conception of the instrument. Over the span of several months, modifications had to be made to sample accurately.

4.3.1 DCFH working solution issues

The initial conception of the instrument involved the use of DCFH working solution as the collection liquid for the mist chamber, reducing the need for mixing of a dilute sample in a separate step and adding analytical time to each cycle. The DCFH working solution was used in place of dI in the mist chamber, which was shielded with aluminum foil. Over time, it became apparent that losing the ability to see the operation of the mist chamber allowed air flow problems to persist. Additionally, before the water trap was introduced, a 2 μm pore size Zefluor filter, of the same type used in the ROS phase selection valve was used instead to reduce the pressure drop across the system and improve airflow. It was not immediately apparent that this filter was unable to retain sufficient liquid in the mist chamber, which meant that the water passed into the mass flow controller, rendering it unable to maintain an appropriate flow. These challenges led to moving the combination of DCFH with a sample to after the collection of particles in dI within the unshielded mist chamber, as has been previously described. Furthermore, it appeared that there was smearing between samples due to the adherence of the DCFH solution and the buffer salts to the top hydrophobic filter and inability to completely rinse and drain the mist chamber. Removing the working solution from the mist chamber reduced many of these physical problems.

4.3.2 Hydrophobic filter

The initial hydrophobic filter used in the filter pack attached to the mist chamber proved to be insufficiently hydrophobic and was allowing a large quantity of liquid over time to pass through the mist chamber and into the vacuum line – specifically, into the

mass flow controller prior to the introduction of a water trap between the mist chamber and mass flow controller. Overloading the controller with liquid caused a reduction in actual flow to the mist chamber, while readings form the device did not change. In higher particulate loading situations the more hydrophobic and smaller pore size (1.0 μm) filter could become rapidly closed with insoluble particulate, causing a pressure drop that precluded the mass flow controller from allowing 17 lpm to the mist chamber in the course of a 24 hour period. More consistent monitoring and changing of this filter generally solved this problem, since the mist chamber available for this study were tested to have a noticeably reduced collection efficiency at flow rates under 15 lpm, as shown above.

4.3.3 Light source degradation

Over the summer and fall of 2011, calibration slopes for the mist chamber decreased slowly without relationship to DCFH working solution viability or age of peroxide standards. It became apparent that the loss of sensitivity and slope was occurring at the same time as a falloff in the dI signal, found in between sampling and used a surrogate for overall system stability. The light intensity values at 530 nm fell off for the primary light source to under 1000 counts before the discovery. A spare identical light source replaced the first, but experienced similar problems rapidly. LED light sources are known to lose intensity slowly at a generally linear rate over a long period of time, a facet of design that is problematic in situations where carefully controlled light intensity is critical. With increasing light intensity, we see increased fluorescence. A new light source with excitation wavelength of 470 nm was purchased through Ocean

Optics (LLS-470). This light source has a dial for the adjustment of voltage to the bulb, which allows for adjustment of light intensity.

4.3.4 Assessment of ROS(g) removal via denuders

Several different compounds were assessed as dry scrubbers or as annular denuder coatings for use in ROS(g) removal to improve the mist chamber collection method for ROS(p) collection. While a dry MnO_2 and a Ti(IV) were considered, only MnO_2 slurry coated annular denuders were evaluated sufficiently to discuss.

Further examination of the denuder efficiency was conducted after the final ROS instrument format was resolved. The ROS phase selection valve was modified to switch between a denuded and undenuded sample, while the filter that had previously been in line for that valve was moved upstream such that the airflow was constantly filtering out particles (i.e., these tests focused solely on ROS(g)). Preliminary, short-term data from the most likely ROS(g) removing agent, MnO_2 in a slurry form, coating annular denuders (URG) showed only between 20% and 54% ROS(g) removal, which may have been limited by low and variable ROS(g) concentrations overall. A partial set of data on Carulite, a dry MnO_2 reagent, packed into a diffusion dryer, showed 45%-66% under similar conditions. Overall ROS(g) measurements taken during this time period were very low, ranging from below the limit of detection (0.025 nmol/m^3) to 1.28 nmol/m^3. This low removal rate and lack of consistency suggested that these denuders would not be effective in removing sufficient and consistent levels of ROS(g) to make worthwhile improvements on ROS collection via a mist chamber. This conclusion led to the use of the difference method for determining ROS(p) from the total ROS signal and the filtered,

or ROS(g) signal, measured in alternating fashion. This method is discussed in detail in Section 4.3.1.

4.4 Preliminary field testing of instrument

The ROS mist chamber instrument was evaluated for ambient sampling by deploying at the Southeastern Aerosol Research and Characterization (SEARCH) network Jefferson Street site during the month of February, 2012. Located in central urban Atlanta, GA the site is considered representative of urban Atlanta (Hansen, Edgerton et al. 2006). The instrument was deployed during February as shown below in Figure 4.4-1 in order to evaluate its operation for an extended period of time. Atmospheric Research and Analysis (ARA) operates a suite of instruments at this site and provided continuous ozone, $PM_{2.5}$, OC and EC data for comparison.

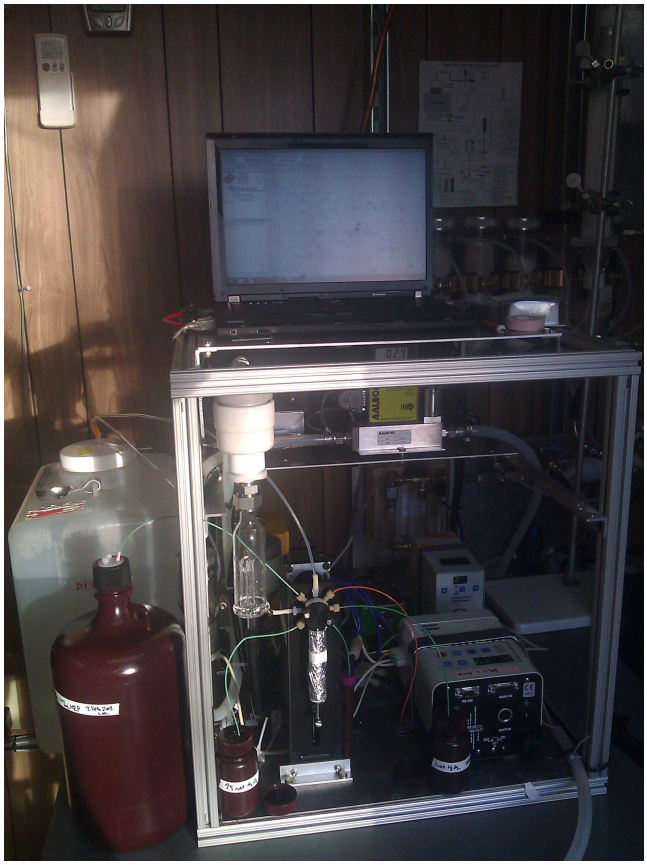

Figure 4.4-1: Image of the deployed ROS instrument at the Jefferson Street field site.

ROS concentration data were collected from February 7 to March 2, 2012. The ROS instrument was operated as previously described, by making a series of alternating ROS(g) and ROS(p+g) measurements as previously described by using the along with blanks to correct for auto-oxidation. An example of the raw data time series is shown.

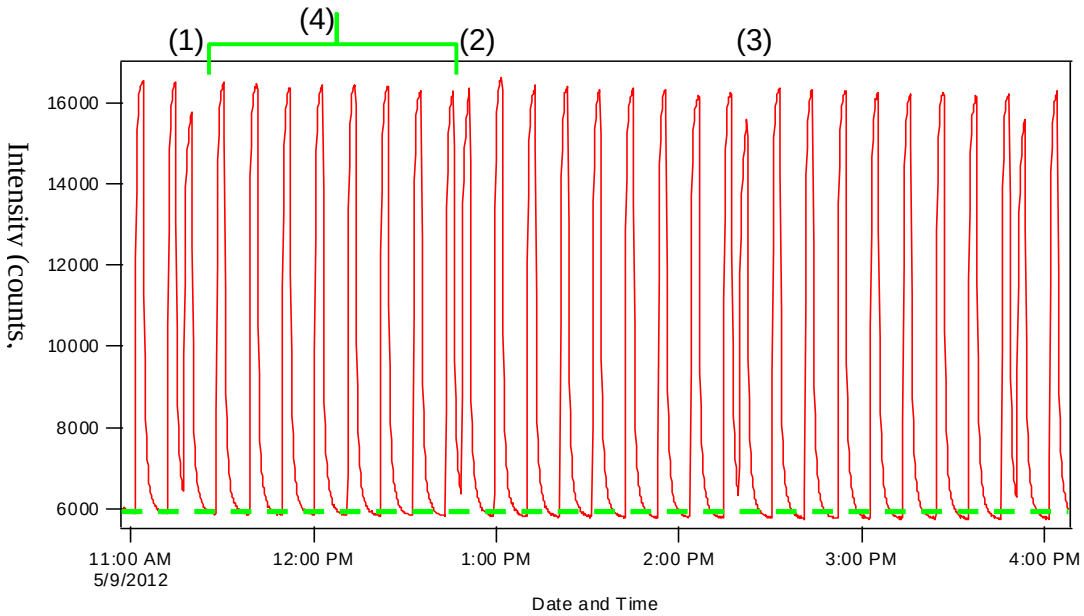

Figure 4.4-2. Time series of raw spectrometer data for ambient ROS. The peaks denoted in (1) and (3) show 'blank', or auto-oxidation measurements, while the peak shown in (2) is a standard measurement. Peaks in between (1) and (2), denoted by (4) for example, are ambient measurement: the first peak is a total ROS measurement, the second an ROS(g) measurement, and alternating so forth.

During this deployment and in the May phase of the later deployment, it was determined that there was a backpressure issue in the syringe pump that contaminated standard measurements taken using the second standard position, and so those values were not used. Only one standard was used from that point on.

4.4.1 Calculation of ROS(p)

In order to accurately subtract the gas phase measurements (ROS(g)) from the total measurements (ROSp+g), the difference between a blank-corrected proceeding ROS(g) measurement and the immediately following ROS(tot) measurement is averaged with the difference between that same ROS(tot) measurement and the following ROS(g)

measurement , resulting in a particle concentration determination for each total measurement made, or

$$\mathrm{ROS(p)_i} = \frac{[ROS(tot)_i - ROS(g)_{i-1}] + [ROS(tot)_i - ROS(g)_{i+1}]}{2}$$

where i represents the number in the series of consecutive ROS measurements.

In the case of the February deployment, both gas and total measurements were very similar, as shown in Figure 4.4.1-1 as an example. The comparable magnitude of these two values (ROS(tot) and ROS(g)) presents difficulty when attempting to use the measurements to ascertain the concentration in the particle phase alone.

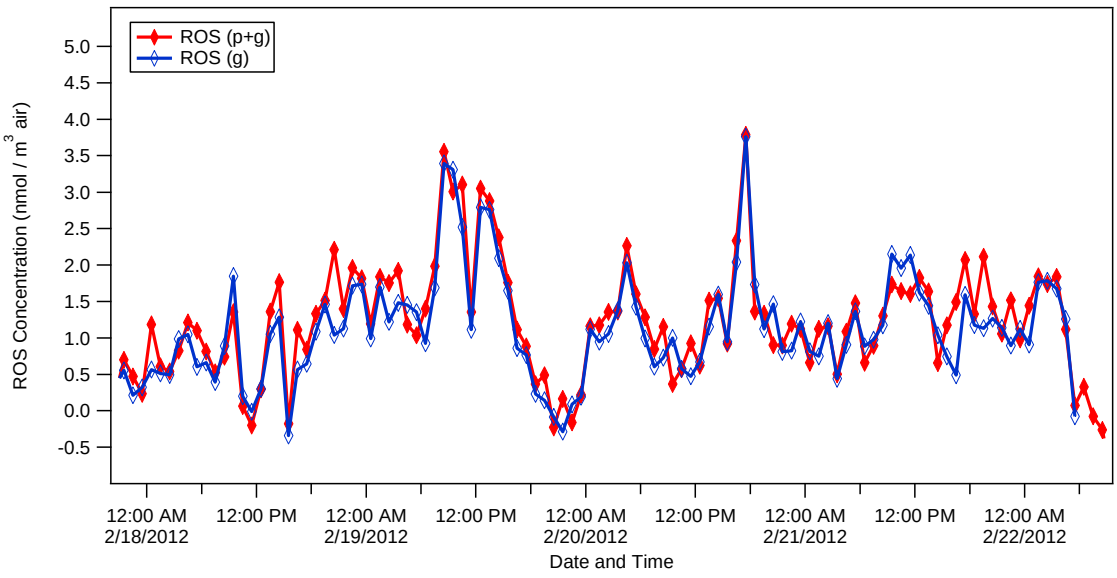

Figure 4.4.1-1. ROS(p+g) and ROS(g) measurements at Jefferson St., February 18-22, 2012.

4.5 Field deployment during SCAPE Project 1: Summer 2012

The mist chamber-ROS instrument was deployed alongside a complement of instruments as part of the Project 1 (measurement phase) of the Southern Center for Air Pollution and Epidemiology. During the first cycle of measurements, one set of instruments was deployed in a trailer at the Jefferson St. SEARCH site in midtown Atlanta for May 2012, then moved to the SEARCH rural background Yorkville site, approximately 80 kilometers northwest of Atlanta for June and shown below in Figure 4.5-1, and then to the rooftop monitoring site at Georgia Tech (midtown Atlanta, only 500 meters from a major highway) during July 2012.

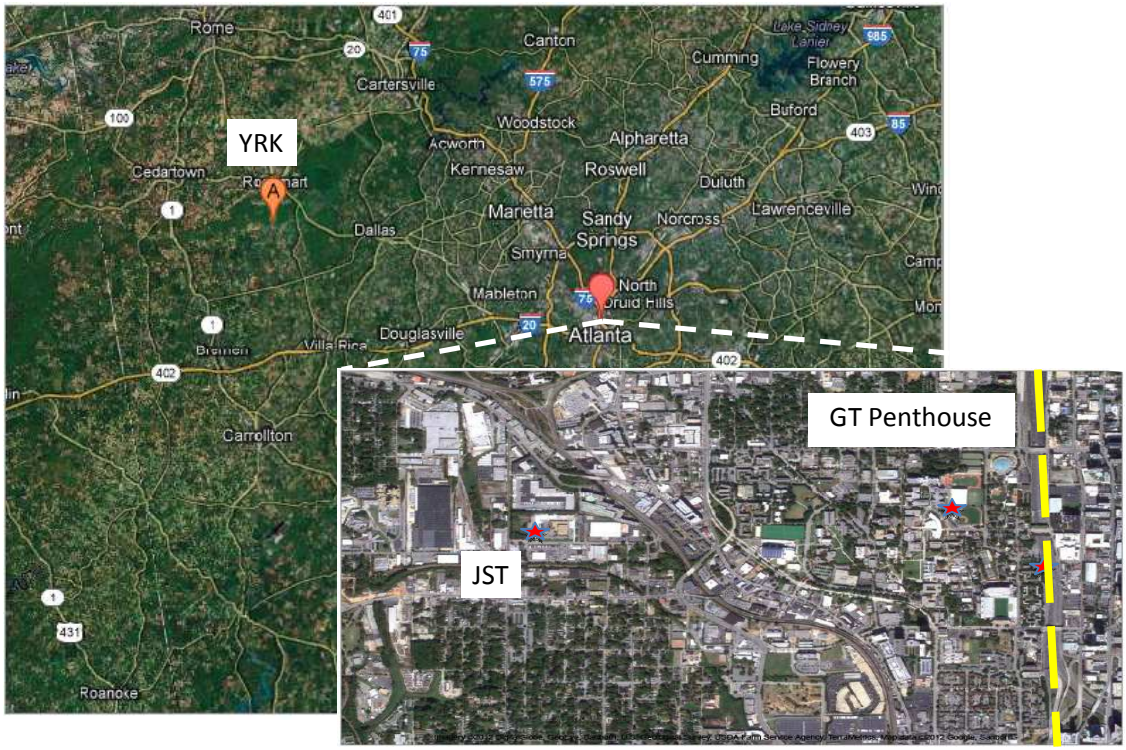

Figure 4.5-1: Map of SCAPE monitoring sites.

Figure 4.5-2: Trailer containing SCAPE instruments, including the mist chamber-ROS device. The structure on the right houses the equipment permanently stationed at Jefferson St. for SCAPE, while the building in the background houses the SEARCH monitoring equipment.

During May and June, the ROS instrument was operated using a 5 minute sampling period in the trailer shown in Figure 4.5-2. During July, in the interests of increasing the particle signal over the gas signal, the sampling time was increased up to 30 minutes. Figure 4.5-3 below shows the time series of particle concentrations as measured at each location. In each graph, all ROS(p) values below the determined LOD for that site were replaced with one half of that value to provide a clear yet positive baseline for the measurements.

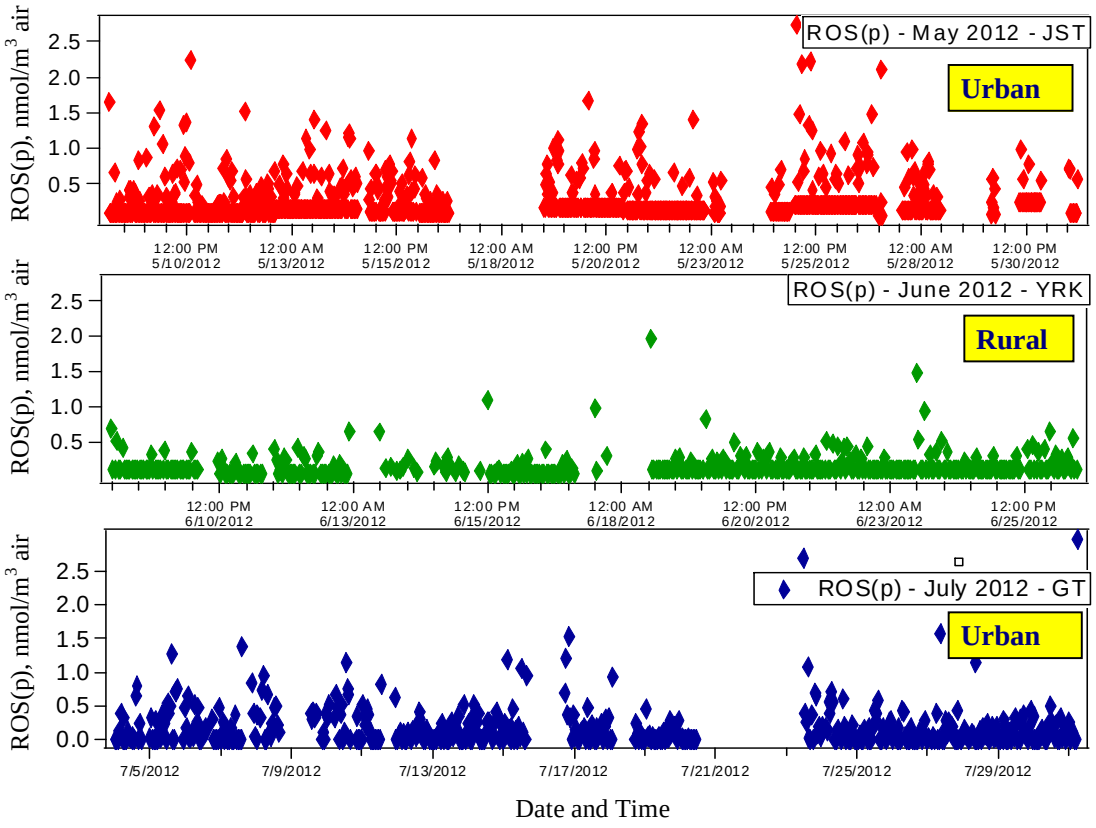

Figure 4.5-3: Time series plots of ROS(p) at various sites. Top, Jefferson Street, JST, an urban location. Middle, Yorkville, YRK, a rural location. Bottom, Georgia Tech, GT, an urban location.

4.5.1 Discussion of ROS(p) data

The subtraction method required for the online instrument to generate particle data led to a large operational LOD given frequent and substantial negative values resulting from this calculation. Due to the necessity of measuring ROS(p) by the difference method, an alternative LOD was determined for conservative use in evaluating which ROS(p) values as concentrations were truly above the limit of detection. Once ROS(p) was determined by subtraction for a study period (per site) and after basic quality control on erratic highs or lows removed erroneous measurements, the LOD for the particle measurements was set to be the standard deviation of all negative values

calculated from the difference method detailed in Section 4.4.1. This value averaged 0.15 nmol/$m^{3,}$ much higher than the LOD determined for the direct measurements,. The high LOD coupled with the variable and high ROS(g) concentrations further emphasizes the importance of reducing or eliminating that gas signal from the particle measurement. If a difference method is to be viable, gas removal via some sort of consistent and effective denuder must be employed. It may be that annular denuders are not as effective as some other gas removal denuder for ROS(g), given the high percentage of ROS in the gas phase shown in this study.

For all monitoring sites, the majority of measurements of ROS(p) were values below the limit of detection of the device (20-27% measurements above LOD). While the LOD for the particle measurement is higher than that of the direct measurements, previous filter studies, particularly those in the summer, suggested that concentrations should be higher than those observed even at the best of times (Venkatachari, Hopke et al. 2005; Wang, Hopke et al. 2011) While there is no data on transition metals at this point for these sites, no site with the exception of the Georgia Tech penthouse lab had proximity to a combustion source, namely the 16-lane highway 500' to the east. This site was additionally elevated at 5 stories above ground level, which could have had a reducing impact on road sources for ROS.

Some chamber studies have shown that in an environment with a higher VOC (linalool) concentration (106 ppb) coupled with lower ozone levels (34-50 ppb) results in the lower ROS production, as opposed to the higher ROS concentrations measured when ozone was much higher (110-150 ppb) but initial linalool concentrations were low (24-32 ppb) (Chen and Hopke 2009) A similar study showed that 'fresh' (ambient) ROS

decreased with increasing biogenic VOCs (Chen, Hopke et al. 2011) though with an increase relative to SOA mass, but further concluding that 'fresh' ROS was lower in ozone limited regions. While drawing a direct line between a chamber study at the southeastern US summer atmosphere is tenuous at best, it does suggest that this particular environment might be a contributing factor to lower than expected ROS concentrations. For this study period, ozone concentrations were not high – ozone did not exceed 100 ppb even in the heat wave at the beginning of July, and averaged around 40 ppb in the urban areas, 60 ppb in the rural background site (consequentially the hottest month of the summer), and it can be expected that in the summer in this region, BVOCs were high, especially isoprene. If nothing else, it seems that there must be a significant sink for ROS in this region during the summer.

4.5.2 Comparison of online system with filter measurements

Online measurements are generally expected to be improvements over offline methods, particularly filter based collections, in that they eliminate many sampling artifacts. In order to better understand the capability of this existing online ROS instrument, its measurements were compared to other online and offline studies of ROS(p). A side-by-side filter study was conducted in July 2012 while the instrument was deployed at the Georgia Tech site. Over a period of 16 days, all weekdays, 1 μm polycarbonate filters (Nuclepore, Whatman) sampled PM at a flow rate of approximately 45 lpm during the operation of the online ROS instrument. Upon completion of sampling the filters were immediately extracted into 30 mL of the same batch of DCFH working solution used in the online instrument, mechanically shaken using a wrist-action shaker

for 15 minutes and analyzed using an identical setup to the online system. This procedure deviated from other studies' filter measurements (Hung and Wang 2001) in two ways: one, the same volume of DCFH was used for each filter, and two, filters were shaken rather than sonicated to extract the particles into solution. The online system also uses the same volume of reagent each time, so these similarities assist in comparing the offline and online data. The filters were not sonicated as at least one study (Hasson and Paulson 2003) suggested that sonicating filters could actually generate more ROS in solution. The mechanical wrist action shaker (Model 70, Burrell Scientific, Pittsburgh, PA, USA) was employed as an alternative particle extraction method. Filter blanks and water blanks were also measured for calibration controls, and standards were checked routinely. A summary of the online ROS(p) for the three months and the period of filter measurements is shown below in Table 4.5.2-1. Studies published previously that measured ROS(p), all on filters, with the exception of the last study (Wang, Hopke et al. 2011), are shown for comparison in Table 4.5.2-2.

Table 4.5.2-1: Comparison of average and span of online and offline ROS(p) measurements during summer study period

.

Month/Location	ROS(p) Average (nmol/m3)	Range (nmol/m3)	Standard Deviation
May 2012 *(JST) (N = 998)*	0.26	0.04 – 2.74	0.33
June 2012 *(YRK) (N=439)*	0.14	0.07 – 1.95	0.19
July 2012 *(GT) (N=512)*	0.24	0.15 – 2.97	0.29
July 2012 *(GT) - filters (N=19)*	0.15	0.05 – 0.34	0.079

Table 4.5.2-2: Comparison of previous ROS(p) studies

Location	Dates	Range (nmol/m3)
Flushing, NY	Jan-Feb 2004	0.87 ± 0.18
Singapore (roadway)	December 2005	15.10 ± 0.10
Singapore (ambient)	December 2005	5.71 ± 2.30
Taipei (Taiwan)	July-Dec 2000	0.54 ± 0.40
Rubidoux, CA	July 2003	5.90 ± 1.70
Rochester, NY	Aug 2009	8.30 ± 2.19

The initial plan for the filter comparison with the online measurements was to compare each individual filter sample with the subsequent online measurement period to see how well these points agreed. However, the majority of the online measurements were comprised of values at or below the LOD, even if the averages for those time periods were influenced by one or a few measurements above that concentration.

Previously an online method was assumed to be inherently superior to filter collection and analysis for these species, though it must be noted that in the field testing of the only other known online ambient ROS monitor (Wang, Hopke et al. 2011) the filter comparisons made to validate the instrument were also observed to at times be higher than online measurements. Here filter measurements also tend to agree with the online results, though the concentrations observed in Atlanta in the summer are of an order of magnitude less than those observed for the week the PILS-ROS system measured in Rochester (Wang, Hopke et al. 2011). The majority of filter measurements shown in Table 4.5.2-2 are higher in concentration than those measured via the mist chamber apparatus, with the exception of the Taipei study.

4.5.3 Analysis of potential ozone interference

Some concerns have been raised over the potential for ozone to interfere with the measurement of ROS when using a mist chamber or similar wet collector. While the mist chamber is unlikely to collect ozone effectively as the K_H of ozone (0.011 M/atm) (Kosak-Channing and Helz 1983) is substantially lower than the minimum typically required for effective collection (10^3 M/atm), the potential interference was still assessed. An ozone primary standard generator (Thermo Environmental Instruments, Model 49S) was used in combination with zero air to generate a sufficient flow to operate the mist chamber with known concentrations of ozone. This supplied gas flow was split and measured additionally by an ozone analyzer to confirm concentrations. Table 4.5.3-1 below shows the effect that typical ozone concentrations had on the activity of the DCFH solution.

Table 4.5.3-1: ROS and ozone concentrations.

Ozone Concentration (ppb)	ROS Response (nmol / m3 air)
60	0.4
60	0.49
100	0.23
105	0.23
133	-0.61
142	0.18
176	-0.43
182	-0.73

In the potential alternate operation of the mist chamber wherein DCFH working solution could be used inside the mist chamber, this experiment would need to be

repeated to verify if, and if so to what extent, ozone might interfere directly with the probe.

CHAPTER 5

CONCLUSIONS AND FUTURE WORK

The fluorescent probe DCFH is an effective analytical method for the determination of ROS in the atmosphere. While its preparation and storage are nontrivial, its sensitivity and repeatability as well its strong record of use in both cellular and particulate assessments of ROS concentrations make it a good tool for measuring atmospheric exogenous ROS. Cost effective equipment exists to construct a viable field instrument for the semi continuous measurement of total ROS provided that adequate quality controls for hardware and chemical components are employed. The analytical backend of the field instrument as described is a rapid and sensitive methodology for measuring ROS in the liquid phase, and would be more effective when coupled with a more efficient means of collecting ROS in the field, such as a device employing a particle concentrator. It has proven difficult to sample ROS in the particle phase due to the difficulties of including the gas phase signal in mist chamber measurements, and the large gas phase concentrations leading to large uncertainties when subtracting those concentrations from total (gas plus particle) measurements.

During the field deployment of the instrument, concentrations of ROS(p) were higher in urban areas than in rural ones, averaging 0.25 nmol H_2O_2 equivalents / m^3 air for urban Atlanta in May and July, and 0.14 nmol/m^3 air for Yorkville during June. These concentrations were comparable to the filter measurements made in Atlanta in July. Online measurements were above the detection limit approximately one quarter of the time. Determining ROS(p) using a difference method proved challenging due to the current inability to remove the gaseous phase prior to collection.

APPENDIX A:

STANDARD OPERATING PROCEDURE FOR MIST CHAMBER-ROS INSTRUMENT

Reactive Oxygen Species (ROS) – Mist Chamber Collection Method
Standard Operating Procedure

I. Scope and Applicability

This SOP describes the operation of the field instrument designed to measure reactive oxygen species (ROS) either as a total (particle+gas) or gas fraction in the atmosphere by collecting soluble ROS compounds with a mist chamber and analyzing the reaction of that liquid with DCFH, via measurement of the fluorescence of the reacted DCFH solution at 530 nm.

II. Summary of Method

Water soluble gases and particles are collected in a mist chamber, wherein a vacuum pump pulls air through a PM2.5 cyclone and through a nebulizing nozzle inside the chamber. The water within the chamber is nebulized and mists within, refluxing down the walls of the chamber. After a set period of time a portion of the liquid is withdrawn using a syringe pump, wherein it is combined with a working solution of DCFH and peroxidase from horseradish (HRP). This solution is pumped from its vial through a flow cell attached to a spectrometer. The solution is excited at 470 nm with an LED light source, at which point is fluoresces at 530 nm. The intensity at 530 nm is measured and compared to a calibration curve to convert relative intensity into actual ROS concentration. The mist chamber is cleaned briefly and reset, making a 15 min integrated measurement every 25 minutes. A valve controls the filtration of the airstream, allowing for the measurement of either total ROS (p+g) or

gas phase only. Every 6 measurements a blank is assessed to correct for auto oxidation of DCFH, using dI instead of mist chamber solution.

WARNING

DCFHDA and DCFH are light sensitive. At no point in time should they be exposed to ambient lighting, either for storage or during use. Both compounds should be kept in the freezer and refrigerator, respectively, when not in active use.

III. Procedure

A. Media Preparation

1. Base solution: DCFHA in ethanol

Materials

250 mL amber bottles

HPLC grade ethanol (Sigma Aldrich)

DCFHDA (Calbiochem, CAS# 4091-99-0)

Graduated cylinders (50 mL)

Scale

Weigh paper

Darkroom and red light

Parafilm

Labels/tape

Procedure

Measure 40 mL of ethanol. Remove the DCFHDA from the freezer. In the darkroom, remove the DCFHA vial from its storage box and black bag. Dissolve 0.0196 g DCFHDA into 40 mL ethanol inside a 250 mL amber bottle. Cap, shake to dissolve, and wrap the lid tightly with Parafilm. Label, data and store in the freezer until use. These solutions may be used for at least 1 month.

2. Working solution: 10 µM DCFH + 1 unit/mL HRP (4L)

Materials

Bottle of DCFHDA in ethanol, prepared as above

0.01 N NaOH (0.4 mL 50% w/w NaOH in 2 L dI)

Na_2HPO_4

NaH_2PO_4

Horseradish from peroxidase, type I (Sigma Aldrich)

Darkroom

Scale

Spatulas/scoopulas

Weigh paper and dishes

dI (bulk and squirt bottle)

2 L volumetric flask

Stirbar (for 2L flask)

1 L volumetric flask

4 L amber carboy jug (VWR)

Replacement cap with holes (fits amber jug)

Funnel

Timer

optional: pH meter

Procedure

Remove a bottle of DCFHDA in ethanol from the freezer. Inside the darkroom, add 160 mL 0.01 NaOH. Recap, invert, start countdown timer for **30 minutes**. Set aside.

Fill a 2 L volumetric flask with dI. Pour out ~400 mL. Add stirbar. Dissolve buffer salts as follows into flask:

10.094 g Na_2HPO_4

3.318 g NaH_2PO_4

Use squirt bottle to rinse salts off side of flask neck. Place flask on stirplate, turn on.

Fill 1 L volumetric flask with dI. Add to 4 L amber carboy jug, using funnel if necessary. Refill with 1L dI. Add most, reserve some to rinse funnel later. Place both inside darkroom.

Shortly before 30 minutes have elapsed, weigh HRP. Each HRP lot may have a different number of purpogallin units (units) per mg, so check each time a new bottle is used. The correct number of units is 1 unit/mL, or 4000 units / 4L. For 52 units/mg, that would be 0.1538 g HRP. Add to flask of buffer salts. **Return HRP immediately to refrigerator**.

When timer indicates 30 minutes, enter darkroom and add contents of DCFHDA-ethanol-NaOH bottle to the 2L buffer salts flask. Add dI to amber bottle to rinse, pour rinse solution into 2L flask. Use squirt bottle to fill 2L to 2L. Turn off stirplate, pour contents carefully into amber jug **using the funnel**. Pour remaining dI from the 1L flask into the funnel to rinse. Cap jug with the replacement hole cap, cover holes with tape. Label jug with contents, date and time of creation. Store in refrigerator until use. Discard after 2 days. (3 days if it spends most of its time in the fridge.)

Glassware may be cleaning by repeated rinsing and soaking in dI (at least 3 rinses and a 2 hour soak) prior to reuse. Plastics may be soaked in the tapwater-Alconox bin prior to a tap and dI rinse and dI bin soak.

B. Instrument Operation

Setup:

Prior to initial operation:

- Fill the dI carboy.
- Empty the waste carboy.
- Place DCFH container in line and insert tubing.
- Place H2O2 standard in line in appropriate port.
- Change the mist chamber hydrophobic filter (1 μM, Tefsep).
- Change the particle filter (2 μM, Zefluor).
- Check debubbler for contamination.
- Check tubing for wear, breaks, etc.
- Check connections for leaks.

Startup:

1) Turn on the peristaltic pump. Observe water flowing out of the flow cell.

2) Start Spectrasuite on laptop. Adjust settings to an integration time of 500 msec and 10 scans to average. BEFORE turning on the light source, save the dark spectrum and subtract it from the spectra.
3) Turn on the light source. Allow to warm up for 10 minutes.
4) Open a stripchart. Record intensity at 530 nm, saved every 15 seconds.
5) Adjust voltage knob to get the intensity of the dI signal to measure around 6000 counts. The knob is very sensitive.
6) Start Kloehn Control and open the current program for the mist chamber.
7) Run the program.
8) Check air flow rate at cyclone and adjust mass flow controller to get 20 lpm.

IV. Quality Control

General Maintenance

Constantly/as needed

- Watch for Kloehn Control error messages. The syringe pump may stop working. This requires a system reset and restart. Be sure to clear out leftover fluids from stopped stages of the run.

Daily

- Check and record total air flow rate at cyclone. If flow dips below 17 lpm, change the mist chamber filter.
- Check filtered air flow rate at cyclone. If this flow dips below 17 lpm, regardless of total flow, replace the particle filter.
- Empty waste (into a sink) as needed.
- Refill dI as needed.
- Observe and record dI base intensity signal.

Every 2 days

- Replace DCFH working solution. Restart strip chart. Either restart the entire program or make a note of where in the program the DCFH changed.

Weekly

- Adjust dI signal to ~6000 counts (it will fall over time, but should not need adjustment more often – if it begins to fall rapidly, stop system and find contamination.)

Monthly

- Clean lines and flow cell with HCl to reduce mold buildup.

V. Revision History

May 1, 2012

August 1, 2012

APPENDIX B:

PRELIMINARY FINDINGS ON A PILS BASED ROS(p) INSTRUMENT

The PILS is a strong candidate for making purely particle phase measurements. The current primary concerns on its viability are the collection temperature for the particles and the analytical limit of detection for ROS. Partitioning theory for hydrogen peroxide suggests a large fraction of that compound alone will convert to the gas phase given the temperature and liquid water content within the PILS, which might reduce the efficiency of that particle collector for ROS. In addition to the potential difficulties in collecting the particles themselves, the PILS at best would concentrate 16.7 lpm of air into 0.1 mL/min of liquid flow. This is not a significant improvement of collection over the mist chamber, though it does exclude interfering gas signals.

The following setup, nearly identical to the existing instrument but for the use of the PILS in place of the mist chamber, was compared side by side with the existing mist chamber instrument.

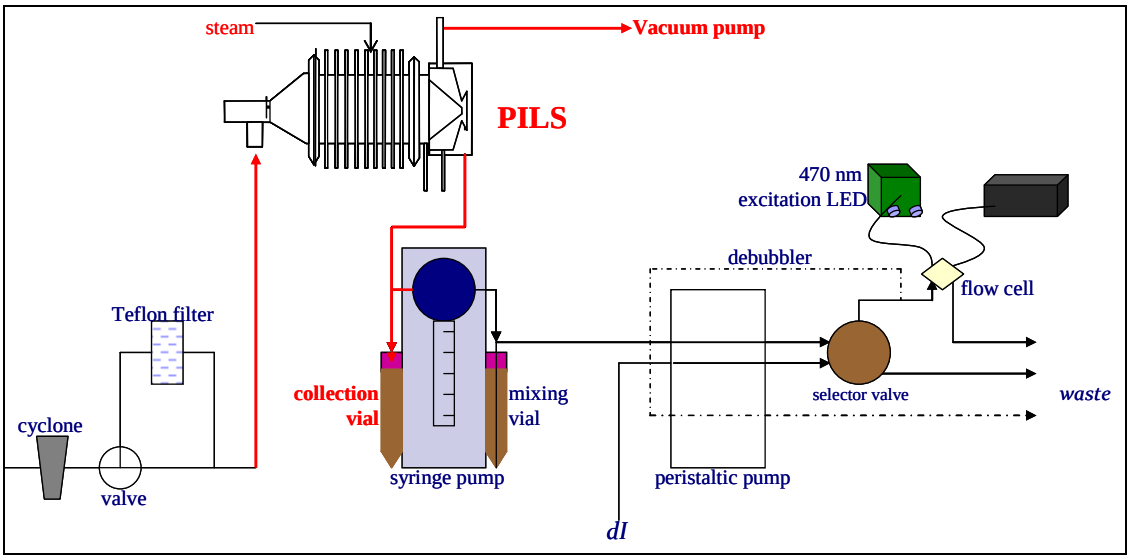

Figure B-1: ROS instrument using a PILS for particle collection.

In this instrument, the mist chamber after the cyclone and ROS phase selector valve is replaced by the particle into liquid sampler (PILS). The design and operation of the PILS is fully described elsewhere (Orsini, Ma et al. 2003). Briefly, the particle laden air stream enters the chamber and mixes with supersaturated steam. The particles are grown and collected via impaction against a quartz impaction plate, where they are rinsed down using a small dI flow. This liquid is collected in a second mixing vial as indicated. The mist chamber automation is modified to withdraw the requisite liquid from this vial as opposed to the mist chamber and is used as previously described. The benefits of this system are that the collection vial will slowly fill during the analysis of the previously withdrawn sample, allowing for collection and analysis in true parallel. The analytical portion of this system is never idle, in fact, since when one sample has been fully analyzed and the mixing vial rinsed, the collection vial has filled with sufficient volume to immediately begin the next cycle.

An instrument of this type was constructed and operated for a brief period of time in March 2012. For the 4 days of continuous measurements, no concentrations above the signal for pure water, or even perceptible variability, were found. Given the limit of detection of 0.28 nmol/L for the analytical system, the PILS system would need to collect 2.8×10^{-13} mol ROS in 1 mL of liquid. If the PILS particle-liquid stream flows on average at 0.15 mL/min and incorporates an ambient airflow of 16.7 L (air) per minute, this indicates that:

$$(2.8 \times 10^{-13} \text{ mol ROS/mL liquid}) * (0.15 \text{ mL liquid/min}) * (1 \text{ min}/16.7 \text{ L air}) * (1000 \text{L air}/1\text{m}^3 \text{ air})$$

$= 1.7 \times 10^{-10}$ mol ROS / m^3 air

[0.17 nmol ROS / m^3 air]

This value is already the conservative determination for LOD of particle measurements from the subtraction method. Since the mist chamber instrument rarely finds these values, it does not seem likely that the PILS apparatus will be an improvement. For reference, the available comparison of the two systems in raw concentrations (including data below the limit of detection for both systems) is shown below in Figure B-1.

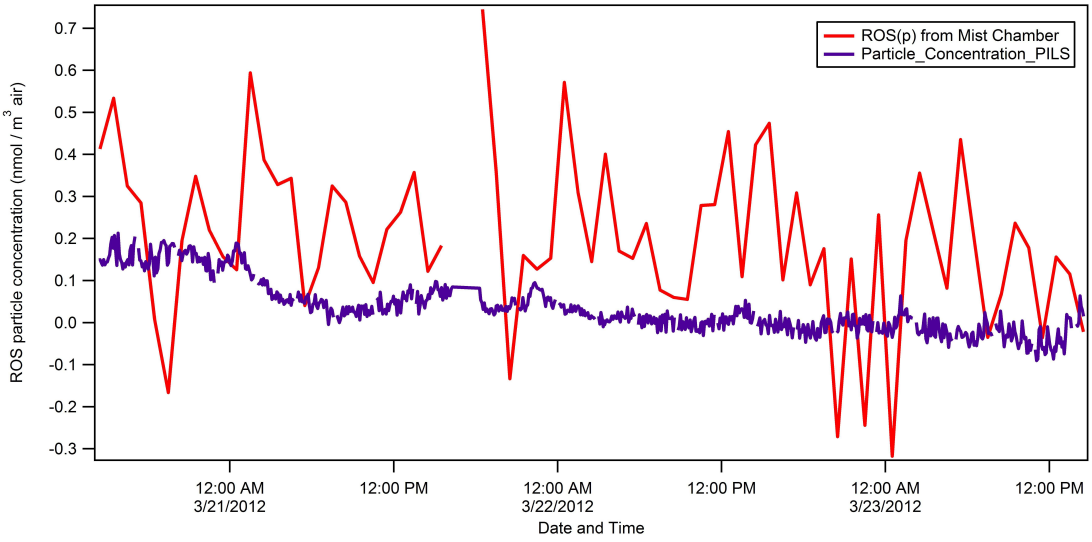

Figure B-2: Comparison between ROS analytical systems paired with a mist chamber and with a PILS.

REFERENCES

Afzal, M., S. Matsugo, et al. (2003). "Method to overcome photoreaction, a serious drawback to the use of dichlorofluorescin in evaluation of reactive oxygen species." Biochemical and Biophysical Research Communications **304**(4): 619-624.

Anderson, C. H., J. E. Dibb, et al. (2008). "Atmospheric water-soluble organic carbon measurements at Summit, Greenland." Atmospheric Environment **42**(22): 5612-5621.

Antonini, J. M., R. W. Clarke, et al. (1998). "Freshly generated stainless steel welding fume induces greater lung inflammation in rats as compared to aged fume." Toxicology Letters **98**: 77-86.

Arakaki, T., Y. Kuroki, et al. (2006). "Chemical composition and photochemical formation of hydroxyl radicals in aqueous extracts of aerosol particles collected in Okinawa, Japan." Atmospheric Environment **40**(25): 4764-4774.

Arellanes, C., S. E. Paulson, et al. (2006). "Exceeding of Henry's Law by Hydrogen Peroxide Associated with Urban Aerosols." Environmental Science & Technology **40**(16).

Ayres, J. G., P. Borm, et al. (2008). "Evaluating the toxicity of airborne particulate matter and nanoparticles by measuring oxidative stress potential--a workshop report and consensus statement." Inhal Toxicol **20**(1): 75-99.

Barrett, W. C., J. P. DeGnore, et al. (1999). "Roles of Superoxide Radical Anion in Signal Transduction Mediated by Reversible Regulation of Protein-tyrosine Phosphatase 1B." The Journal of Biological Chemistry **274**(49): 34543-34546.

Biswas, S., V. Verma, et al. (2009). "Oxidative Potential of Semi-Volatile and Non Volatile Particulate Matter (PM) from Heavy-Duty Vehicles Retrofitted with Emission Control
Technologies." Environmental Science & Technology **43**: 8.

Black, M. J. and R. B. Brandt (1974). "Spectrofluorometric Analysis of Hydrogen Peroxide." Analytical Biochemistry **58**: 246-254.

Cathcart, R., E. Schwiers, et al. (1983). "Detection of Picolmole Levels of Hydroperoxides Using a Fluorescent Dichlorofluorescein Assay." Analytical Biochemistry **134**: 111-116.

Charrier, J. G. and C. Anastasio (2012). "On dithiothreitol (DTT) as a measure of oxidative potential for ambient particles: evidence for the importance of soluble \newline transition metals." Atmospheric Chemistry and Physics **12**(19): 9321-9333.

Chen, X. and P. K. Hopke (2009). "A chamber study of secondary organic aerosol formation by linalool ozonolysis." Atmospheric Environment **43**: 6.

Chen, X., P. K. Hopke, et al. (2011). "Secondary Organic Aerosol from Ozonolysis of Biogenic Volatile Organic Compounds: Chamber Studies of Particle and Reactive Oxygen Species Formation." Environmental Science & Technology **45**(1): 276-282.

Cheung, K. L., L. Ntziachristos, et al. (2010). "Emissions of Particulate Trace Elements, Metals and Organic Species from Gasoline, Diesel, and Biodiesel Passenger Vehicles and Their Relation to Oxidative Potential." Aerosol Science and Technology **44**(7): 500-513.

Cheung, K. L., A. Polidori, et al. (2009). "Chemical Characteristics and Oxidative Potential of Particulate Matter Emissions from Gasoline, Diesel, and Biodiesel Cars." Environmental Science & Technology **43**: 6334-6340.

Cho, A. K., C. Sioutas, et al. (2005). "Redox activity of airborne particulate matter at different sites in the Los Angeles Basin." Environ Res **99**(1): 40-47.

Cofer III, W. R., V. G. Collins, et al. (1985). "Improved Aqueous Scrubber for Collection of Soluble Atmospheric Trace Gases." Environmental Science & Technology **19**(6): 557-560.

Cofer III, W. R. and J. Edahl, Robert A. (1986). "A New Technique For Collection, Concentration and Determination of Gaseous Tropospheric Formaldehyde." Atmospheric Environment **20**(5): 979-984.

Cohn, C. A., S. R. Simon, et al. (2008). "Comparison of fluorescence-based techniques for the quantification of particle-induced hydroxyl radicals." Particle and Fibre Toxicology **5**(2): 9.

DiStefano, E., A. Eiguren-Fernandez, et al. (2009). "Determination of metal-based hydroxyl radical generating capacity of ambient and diesel exhaust particles." Inhal Toxicol **21**(9): 731-738.

Gomes, A., E. Fernandes, et al. (2005). "Fluorescence probes used for detection of reactive oxygen species." Journal of Biochemical and Biophysical Methods **65**.

Hansen, A., E. Edgerton, et al. (2006). "Air Quality Measurements for the Aerosol Research and Inhalation Epidemiology Study." Journal of the Air and Waste Management Association **56**: 14.

Hasson, A. S. and S. E. Paulson (2003). "An investigation of the relationship between gas-phase and aerosol-borne hydroperoxides in urban air." Journal of Aerosol Science **34**(4): 459-468.

Hu, S., A. Polidori, et al. (2008). "Redox activity and chemical speciation of size fractioned PM in the communities of the Los Angeles – Long Beach Harbor." Atmospheric Chemistry and Physics **8**(3): 11643-11672.

Hung, H.-F. and C.-S. Wang (2001). "Experimental determination of reactive oxygen species in Taipei aerosols." Journal of Aerosol Science **32**: 1201-1211.

Jacob, D. J. (1999). Introduction to Atmospheric Chemistry. Princeton, New Jersey, Princeton University Press.

Jakubowski, W. and G. Bartosz (2000). "2,7-dichlorofluorescin oxidation and reactive oxygen species: what does it measure?" Cell Biol Int **24**(10): 757-760.

Kao, M.-C. and C.-S. Wang (2002). "Reactive Oxygen Species in Incense Smoke." Aerosol and Air Quality Research **2**(1): 9.

Klippel, T., H. Fischer, et al. (2011). "Distribution of hydrogen peroxide, methyl hydroperoxide and formaldehyde over central Europe during the HOOVER project." Atmospheric Chemistry and Physics Discussions **11**(1): 289-340.

Kosak-Channing, L. F. and G. R. Helz (1983). "Solubility of Ozone in Aqueous Solutions of 0-0.6 M Ionic Strength at 5-30 C." Environmental Science & Technology **17**: 5.

Kumagai, Y., S. Koide, et al. (2002). "Oxidation of Proximal Protein Sulfhydryls by Phenanthraquinone, a Component of Diesel Exhaust Particles." Chem. Res. Toxicol. **15**(4): 483-489.

Landreman, A. P., M. M. Shafer, et al. (2008). "A Macrophase-Based Method for the Assessment of the Reactive Oxygen Species (ROS) Activity of Atmospheric Particulate Matter (PM) and Application to Routine (Daily-24 h) Aerosol Monitoring Studies." Aerosol Science and Technology **42**: 12.

LeBel, C. P., H. Ischiropolous, et al. (1992). "Evaluation of the Probe 2', 7'-Dichlorofluorescin as an Indicator of Reactive Oxygen Species Formation and Oxidative Stress " Chem. Res. Toxicol. **5**: 5.

LeBel, C. P., H. Ischiropolous, et al. (1992). "Evaluation of the Probe 2‘,7‘-Dichiorofluorescin as an Indicator of Reactive Oxygen Species Formation and Oxidative Stress." Chem. Res. Toxicol. **5**(2): 227-231.

Li, N., C. Sioutas, et al. (2003). "Ultrafine Particulate Pollutants Induce Oxidative Stress and Mitochondrial Damage." Environmental Health Perspectives **111**(4): 455-460.

Liu, H. H., Y. C. Wu, et al. (2007). "Production of ozone and reactive oxygen species after welding." Arch Environ Contam Toxicol **53**(4): 513-518.

Morgan, T. E., D. A. Davis, et al. (2001). "Glutamatergic Neurons in Rodent Models Respond to Nanoscale Particulate Urban Air Pollutants In Vivo and In Vitro." Environmental Health Perspectives **119**(7): 7.

Oberdörster, E. (2004). "Manufactured Nanomaterials (Fullerenes, C60) Induce Oxidative Stress in the Brain of Juvenile Largemouth Bass." Environmental Health Perspectives **112**(10): 1058-1062.

Orsini, D. A., Y. Ma, et al. (2003). "Refinements to the particle-into-liquid sampler (PILS) for ground and airborne measurements of water soluble aerosol composition." Atmospheric Environment **37**(9-10): 1243-1259.

Pope, C. A., M. J. Thun, et al. (1995). "Particulate air pollution as a predictor of mortality in a prospective study of US adults." American journal of respiratory and critical care medicine **151**(3): 669-674.

Reeves, C. E. and S. A. Penkett (2003). "Measurements of Peroxides and What They Tell Us." Chem. Rev. **103**(12): 5199-5218.

Rota, C., C. F. Chignell, et al. (1999). "Evidence for free radical formation during the oxidation of 2',7'-dichlorofluorescin to the fluorescent dye 2',7'-dichlorofluorescein by horseradish peroxidase: possible implications for oxidative stress measurements." Free Radical Biology and Medicine **27**(7/8): 9.

Rothe, G. and G. Valet (1990). "Flow Cytometric Analysis of Respiratory Burst Activity in Phagocytes with Hydroethidine and 2',7'-Dichlorofluorescin." Journal of Leukocyte Biology **47**: 440-448.

Sameenoi, Y., K. Koehler, et al. (2012). "Microfluidic electrochemical sensor for on-line monitoring of aerosol oxidative activity." J Am Chem Soc **134**(25): 10562-10568.

See, S. W., Y. H. Wang, et al. (2007). "Contrasting reactive oxygen species and transition metal concentrations in combustion aerosols." Environmental Research **103**: 8.

Seinfeld, J. H. and S. N. Pandis (2006). ATMOSPHERIC CHEMISTRY AND PHYSICS: From Air Pollution to Climate Change. Hoboken, New Jersey, John Wiley and Sons, Inc.

Shinyashiki, M., A. Eiguren-Fernandez, et al. (2009). "Electrophilic and redox properties of diesel exhaust particles." Environ Res **109**(3): 239-244.

Sioutas, C., R. J. Delfino, et al. (2005). "Exposure Assessment for Atmospheric Ultrafine Particles (UFPs) and Implications in Epidemiologic Research." Environmental Health Perspectives **113**(8): 947-955.

Spaulding, R. S., R. W. Talbot, et al. (2002). "Optimization of a Mist Chamber (Cofer Scrubber) for Sampling Water-Soluble Organics in Air." Environmental Science & Technology **36**(8): 1798-1808.

Squadrito, G. L., R. Cueto, et al. (2001). "Quinoid Redox Cycling as a Mechanism for Sustained Free Radical Generation by Inhaled Airborne Particulate Matter." Free Radical Biology and Medicine **31**(9): 7.

Sugamura, K. and J. Keaney, John F. (2011). "Reactive oxygen species in cardivascular disease." Free Radical Biology and Medicine **51**: 978-992.

Towne, V., M. Will, et al. (2004). "Complexities in horseradish peroxidase-catalyzed oxidation of dihydrophenoxazine derivatives: appropriate ranges for pH values and hydrogen peroxide concentrations in quantitative analysis." Analytical Biochemistry **334**: 7.

Veitch, N. C. (2004). "Horseradish peroxidase: a modern view of a classic enzyme." Phytochemistry **65**(3): 249-259.

Venkatachari, P. and P. K. Hopke (2008). "Development and Laboratory Testing of an Automated Monitor for the Measurement of Atmospheric Particle-Bound Reactive Oxygen Species (ROS)." Aerosol Science and Technology **42**(8): 629-635.

Venkatachari, P., P. K. Hopke, et al. (2007). "Characterization of Wintertime Reactive Oxygen Species Concentrations in Flushing, New York." Aerosol Science and Technology **41**(2): 97-111.

Venkatachari, P., P. K. Hopke, et al. (2005). "Measurement of Particle-Bound Reactive Oxygen Species in Rubidoux Aerosols." Journal of Atmospheric Chemistry **50**: 49-58.

Verma, V., M. M. Shafer, et al. (2010). "Contribution of transition metals in the reactive oxygen species activity of PM emissions from retrofitted heavy-duty vehicles." Atmospheric Environment **44**(39): 5165-5173.

Vidrio, E., C. Phuah, et al. (2009). "Generation of hydroxyl radicals from ambient fine particles in a surrogate lung fluid solution." Environmental Science & Technology **43**(3): 6.

von Schneidemesser, E., E. A. Stone, et al. (2010). "Toxic metals in the atmosphere in Lahore, Pakistan." Sci Total Environ **408**(7): 1640-1648.

Wang, Y., C. Arellanes, et al. (2010). "Probing the Source of Hydrogen Peroxide Associated with Coarse Mode Aerosol Particles in Southern California." Environmental Science & Technology **44**(11): 4070–4075.

Wang, Y., P. K. Hopke, et al. (2011). "Laboratory and field testing of an automated atmospheric particle-bound reactive oxygen species sampling-analysis system." J Toxicol **2011**: 419476.

Wardman, P. (2008). "Use of the Dichlorofluorescein Assay to Measure "Reactive Oxygen Species"." Radiation Research **170**: 3.

Xia, T., M. Kovochich, et al. (2006). "Comparison of the Abilities of Ambient and Manufactured Nanoparticles To Induce Cellular Toxicity According to an Oxidative Stress Paradigm." Nano Letters **6**(8): 1794-1807.

Zhang, Y., J. J. Schauer, et al. (2008). "Source Apportionment of in Vitro Reactive Oxygen Species Bioassay Activity from Atmospheric Particulate Matter." Environmental Science & Technology **42**: 7502-7509.

Zhou, M., Z. Diwu, et al. (1997). "A Stable Nonfluorescent Derivative of Resorufin for the Fluorometric Determination of Trace Hydrogen Peroxide: Applications in Detecting the Activity of Phagocyte NADPH Oxidase and Other Oxidases." Analytical Biochemistry **253**: 162-168.